

RESEARCH PAPER



# Design and green synthesis of novel quinolinone derivatives of potential anti-breast cancer activity against MCF-7 cell line targeting multi-receptor tyrosine kinases

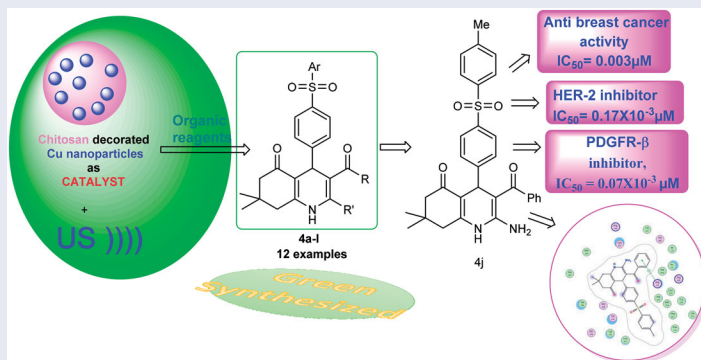
Mohamed Mokhtar<sup>a</sup> , Khadijah S. Alghamdi<sup>b</sup>, Nesreen S. Ahmed<sup>c</sup> , Dina Bakhotmah<sup>a</sup>  and Tamer S. Saleh<sup>d,e</sup>

<sup>a</sup>Chemistry Department, Faculty of Science, King Abdulaziz University, Jeddah, Saudi Arabia; <sup>b</sup>Chemistry Department, Faculty of Science, Albaha University, Albaha, Saudi Arabia; <sup>c</sup>Department of Therapeutic Chemistry, National Research Centre, Cairo, Egypt; <sup>d</sup>Department of Chemistry, University of Jeddah, College of Science, Jeddah, Saudi Arabia; <sup>e</sup>Green Chemistry Department, National Research Centre, Giza, Egypt

## ABSTRACT

A new set of 4,6,7,8-tetrahydroquinolin-5(1H)-ones were designed as cytotoxic agents against breast cancer cell line (MCF-7) and synthesised under ultrasonic irradiation using chitosan decorated copper nanoparticles (CS/CuNPs) catalyst. The new compounds **4b**, **4j**, **4k**, and **4e** exhibited the most potent cytotoxic activity of IC<sub>50</sub> values (0.002 – 0.004 μM) comparing to Staurosporine of IC<sub>50</sub>; 0.005 μM. The latter derivatives exhibited a promising safety profile against the normal human WI38 cells of IC<sub>50</sub> range 0.0149 – 0.048 μM. Furthermore, the most promising cytotoxic compounds **4b**, **4j** were evaluated as multi-targeting agents against the RTK protein kinases; EGFR, HER-2, PDGFR-β, and VEGFR-2. Compound **4j** showed promising inhibitory activity against HER-2 and PDGFR-β of IC<sub>50</sub> values 0.17 × 10<sup>-3</sup>, 0.07 × 10<sup>-3</sup> μM in comparison with the reference drug sorafenib of IC<sub>50</sub>; 0.28 × 10<sup>-3</sup>, 0.13 × 10<sup>-3</sup> μM, respectively. In addition, **4j** induced apoptotic effect and cell cycle arrest at G2/M phase preventing the mitotic cycle in MCF-7 cells.

## GRAPHICAL ABSTRACT



## ARTICLE HISTORY

Received 30 April 2021  
Revised 4 June 2021  
Accepted 12 June 2021

## KEYWORDS

4,6,7,8-Tetrahydroquinolin-5(1H)-one; HER-2 inhibitors; breast cancer; apoptosis; molecular docking study

## 1. Introduction

Breast cancer is one of the most common causes that threatens women's health impacting ~15% of all cancer deaths occurred in women all over the world<sup>1,2</sup>. The incidence of breast cancer is increasing in all the regions of globe. Although chemo and radiotherapies are considered the most important prime option for the treatment of cancer disease,<sup>3</sup> the drug-induced toxicity to the normal cells and drug-resistance constitute problems that still need to be resolved<sup>4</sup>. Therefore, the discovery of new selective and safer anticancer agents is still a great interest in the field of medicinal chemistry<sup>5</sup>.

Receptor tyrosine kinases (RTKs) are transmembrane proteins. They are composed of many triggered domains when a ligand binds to their extracellular regions, activating signalling cascades downstream<sup>6,7</sup>. RTKs such as; epidermal growth factor receptor (EGFR), vascular endothelial growth factor receptor-2 (VEGFR-2), and PDGFR play crucial roles in controlling multiple cellular processes, including cell proliferation, differentiation, survival, and apoptosis. Mutations or deletions in gene functions can result in uncontrolled expression of protein kinases, which can lead to tumour development, angiogenesis, and metastasis. Thus, RTKs are considered novel drug targets to develop tyrosine kinase

**CONTACT** Mohamed Mokhtar  [mmokhtar2000@yahoo.com](mailto:mmokhtar2000@yahoo.com), [mmoustafa@kau.edu.sa](mailto:mmoustafa@kau.edu.sa)  Chemistry Department, Faculty of Science, King Abdulaziz University, Jeddah 21589, Saudi Arabia

 Supplemental data for this article can be accessed [here](#).

© 2021 The Author(s). Published by Informa UK Limited, trading as Taylor & Francis Group.

This is an Open Access article distributed under the terms of the Creative Commons Attribution License (<http://creativecommons.org/licenses/by/4.0/>), which permits unrestricted use, distribution, and reproduction in any medium, provided the original work is properly cited.

inhibitors<sup>6-9</sup>. In addition, these suppressors can inhibit the overexpression of tyrosine kinase and maintain its physiological balance<sup>10</sup>. The US FDA approves more than 60 small-molecule protein kinase inhibitors. Most of them are multi-targeting suppressors synergistically functioning on many signalling pathways by interacting with each target simultaneously<sup>11</sup>. Targeting multiple kinases increases the anticancer potency as well as reduces the risk of developing drug resistance<sup>11-13</sup> (Figure 1).

Quinoline is naturally present in many alkaloids having potent antitumor activity, for example, camptothecin<sup>14</sup> (Figure 1). Quinoline scaffold and its related derivatives represent a broad spectrum of pharmacological activities, especially in drug discovery of new anticancer agents<sup>15-18</sup>. Food and Drug Administration (FDA) has approved various quinoline small molecules acting as protein kinases inhibitors for clinical uses in cancer disease<sup>19-22</sup> (Figure 1). The occurrence of the nitrogen atom in the quinoline nucleus withdraws electrons by resonance and interferes with the equal distribution of  $\pi$  electron density. It has been reported that the quinoline nucleus has a great tendency to bind to the active site of various proteins *via* the formation of hydrogen bonds with its nitrogen atom and  $\pi$ - $\pi$  stacking complexes with complementary amino acid residues<sup>15,16</sup>.

Furthermore, multiple sulphonyl compounds have been reported to inhibit the growth of various human tumour cell lines. Various sulphonamide derivatives, such as HMN-214, E7010 (ABT-751), and E7070 (Indisulam), represented antitumor activity through different various modes of actions as multidrug resistance

down-regulation, inhibition of tubulin polymerisation as well as RTKs inhibition<sup>23-27</sup> (Figure 2).

Molecular hybridisation currently appears as a promising drug design strategy, specifically in discovering new anticancer drugs<sup>28,29</sup>. It has been reported that conjugating of two or more pharmacophores in the same molecular architecture might decrease the risk of drug-drug interactions, overcome the problem of drug resistance as well as enhance the biological efficacy *via* the binding with different targets as one single entity<sup>30</sup>.

Based on the above findings, in continuation of our recent work of using green synthetic approaches to develop a variety of heterocyclic systems with great biological importance<sup>31-34</sup>, and in an attempt to prepare new potent anti-breast cancer leads of potential suppression activity against different RTKs EGFR, HER-2, PDGFR- $\beta$ , and VEGFR-2, this study deals with the synthesis of new tetrahydroquinolines hybridised with other substituted phenylsulfonyl-phenyl moieties at C-4 position and conjugated with different groups at C-2 and C-3 positions (Figure 3). It has been taken in consideration the effect of molecular orientation, ring size variation and the occurrence of different heteroatoms that could provide hydrogen binding with various RTKs binding pockets (Figure 3). The cytotoxic activity against human breast cancer cells (MCF-7) was evaluated for all the new prepared analogues. In addition, *in vitro* multi-targeting inhibition assessment against EGFR, HER-2, PDGFR- $\beta$ , and VEGFR-2 of the most active cytotoxic candidates was also carried out. Extra investigations of different mechanistic pathways such as cell cycle analysis and apoptosis were

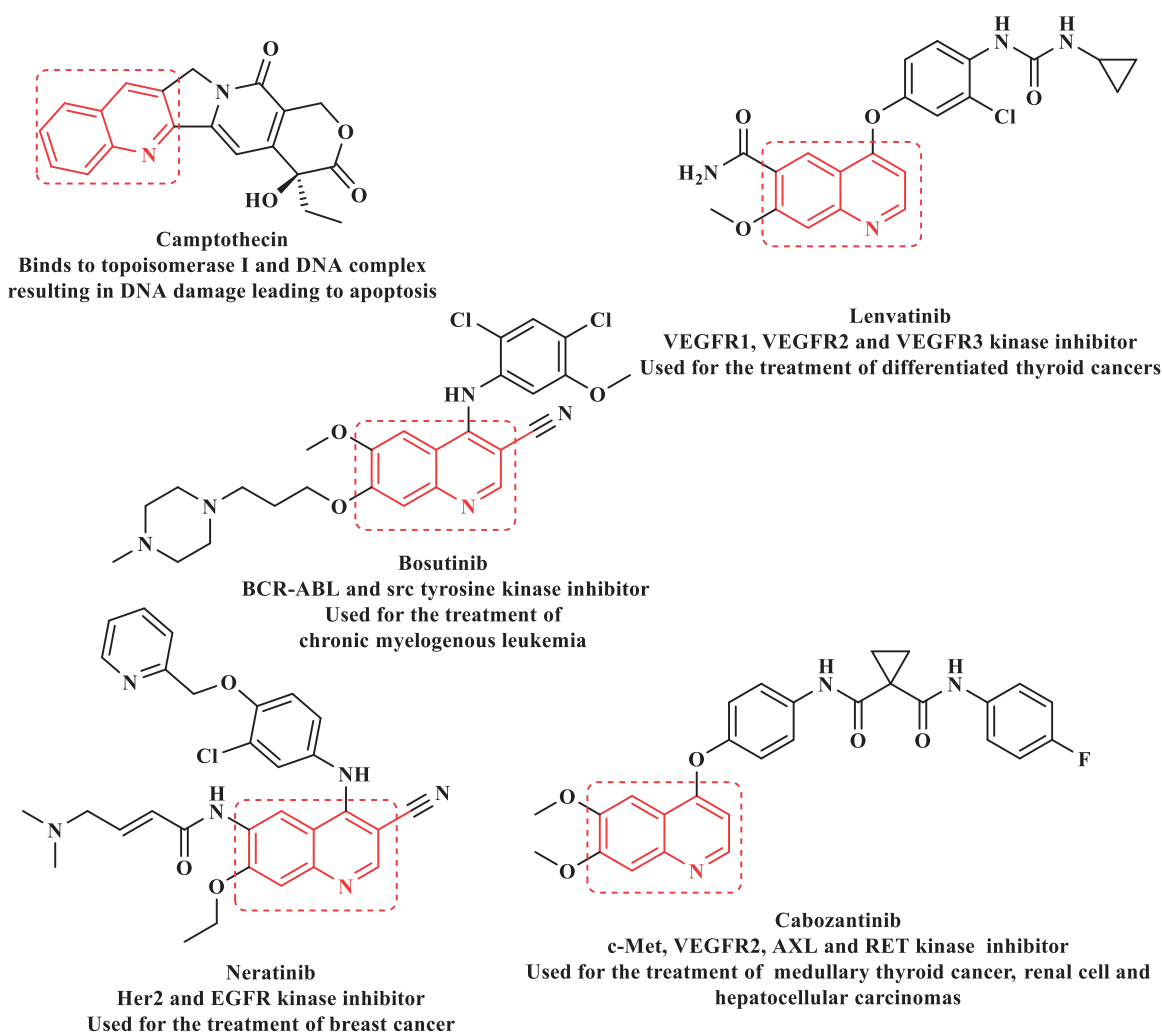


Figure 1. Quinoline-based multi-kinase inhibitors approved by FDA.

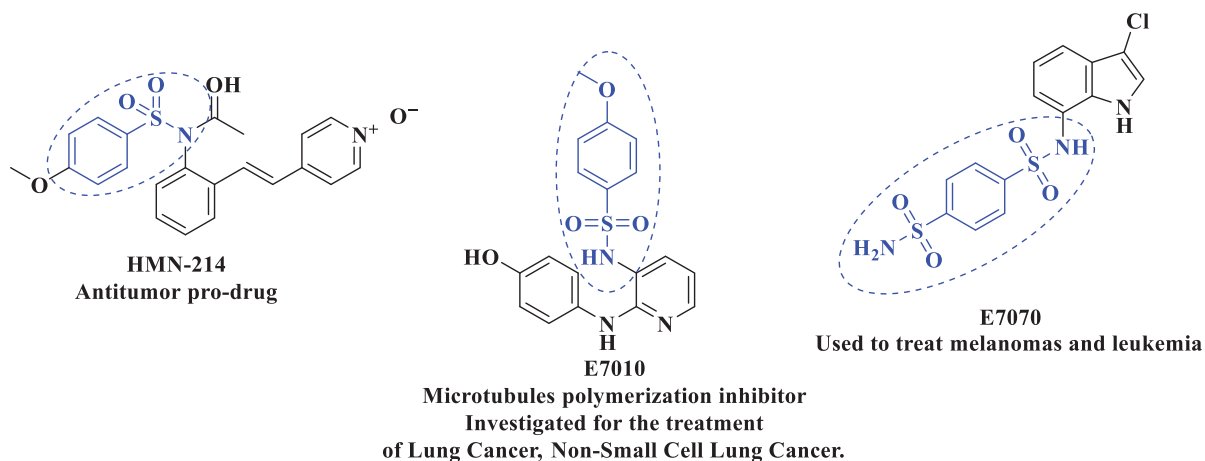


Figure 2. Various sulphonamide candidates of antitumor activity *via* different various modes of actions.

evaluated for the most promising compound as a representative example for the new active analogues. Furthermore, molecular modelling studies were performed to explore the modes of interaction between the promising target compounds and the vital amino acids residues of different kinases to ascertain binding stability and the relationship between their physicochemical characteristics and their favourable suppression effects.

## 2. Materials and methods

### 2.1. Chemistry

All organic solvents were purchased from commercial sources and used as received unless otherwise stated. All other chemicals were purchased from Merck, Aldrich, or Acros and used without further purification. Thin-layer chromatography (TLC) was performed on pre-coated Merck 60 GF254 silica gel plates with a fluorescent indicator, and detection by means of UV light at 254 and 360 nm. The melting points were measured on a Stuart melting point apparatus and are uncorrected. IR spectra were recorded on a Smart iTR, which is an ultrahigh-performance, versatile Attenuated Total Reflectance (ATR) sampling accessory on the Nicolet iS10 FT-IR spectrometer. The NMR spectra were recorded on a Bruker Avance III 400 (9.4T, 400.13 MHz for  $^1\text{H}$ , 100.62 MHz for  $^{13}\text{C}$ ) spectrometer with a 5-mm BBFO probe, at 298 K and a Bruker High Performance Digital FT-NMR Spectrometer Avance III 850 MHz. Chemical shifts ( $\delta$  in ppm) are given relative to internal solvent,  $\text{DMSO-}d_6$  2.50 for  $^1\text{H}$  and 39.50 for  $^{13}\text{C}$ ,  $\text{CDCl}_3$  7.25 for  $^1\text{H}$  and 77.7 was used as an external standard. Mass spectra were recorded on a Thermo ISQ Single Quadrupole GC-MS. Elemental analyses were carried out on a Euro Vector instrument C, H, N, S analyser EA3000 Series. Sonication was performed by Techno-gaz sonicator (with a frequency of 37 kHz and ultrasonic peak max. 320 W).

The catalyst (CS/CuNPs)<sup>35</sup>, 4-(phenylsulfonyl)benzaldehyde (**2a**)<sup>36</sup> and 4-tosylbenzaldehyde (**2b**)<sup>37</sup> were prepared according to reported literature.

### 2.2. General methods for the synthesis of 4,6,7,8-tetrahydroquinolin-5(1H)-one derivatives (4a–l)

#### 2.2.1. Silent reactions

A mixture of dimedone (**1**) (1 mmol), different aldehydes **2a**, **b** (1 mmol), active methylene compounds **3a–f** (1 mmol) and ammonium acetate (9 mmol) in ethanol (25 ml) containing a catalytic amount of Cu-chitosan NPs (0.1 g) was refluxed at 60 °C for the appropriate time (*cf.* Table 1) until completion of the reaction

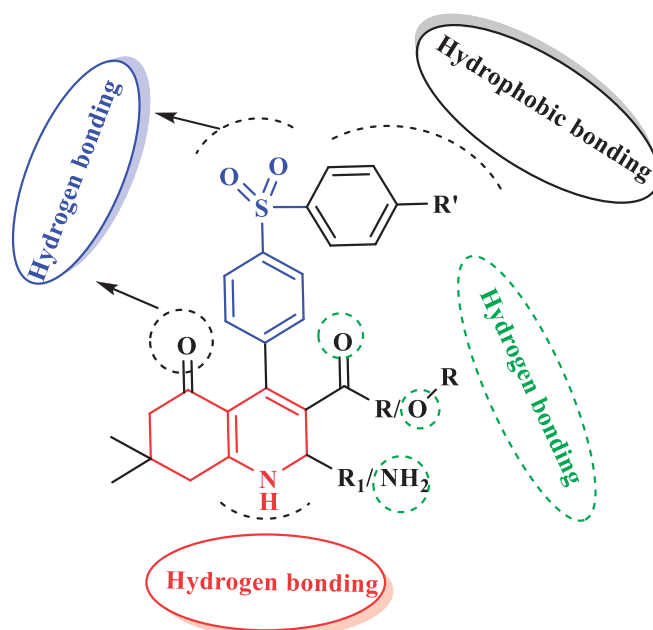


Figure 3. The proposed hypothetic model for the new tetrahydroquinoline – phenylsulfonyl derivatives.

(monitored by TLC). The reaction mixture was filtered to separate the catalyst; then, the filtrate was cooled at room temperature, and the reliable product obtained was filtered, dried, and purified by recrystallisation from ethanol.

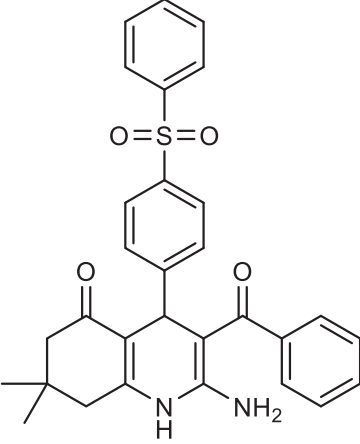
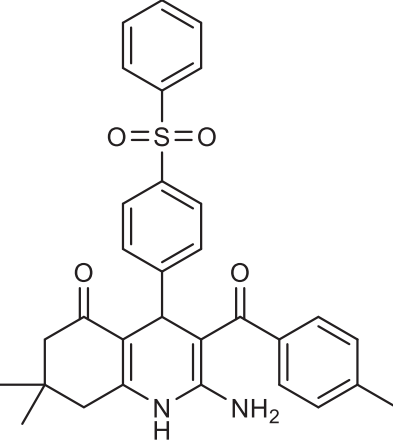
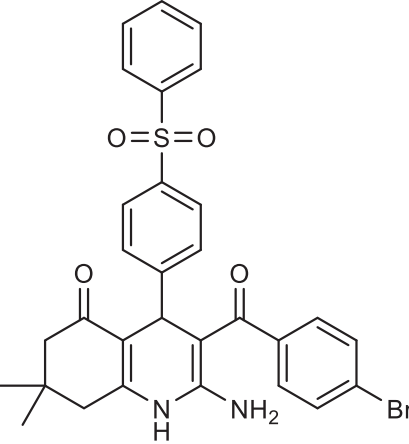
#### 2.2.2. Sonicated reactions

These processes were performed on the same scale described above for silent reactions. All The reactions were kept at 60 °C, which was attained by adding or removing water in an ultrasonic bath (the temperature inside the reaction vessel was 58–63 °C). The sonochemical reactions were continued for a suitable time (*cf.* Table 1) until the starting materials were no longer detectable by TLC. Then, the catalyst was separated, and the products obtained were purified as described above in silent reaction procedures. The synthesised compounds with their physical data are listed below.

##### 2.2.2.1. Methyl 2,7,7-trimethyl-5-oxo-4-(4-(phenylsulfonyl)phenyl)-1,4,5,6,7,8-hexahydroquinoline-3-carboxylate (4a). Mp 260–262 °C.



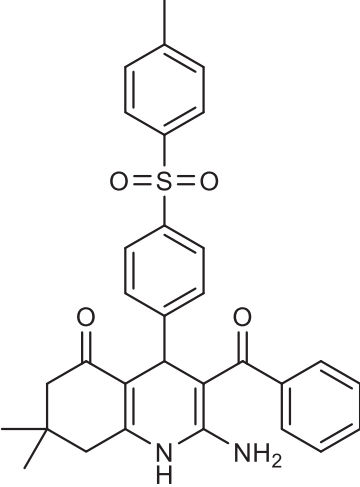
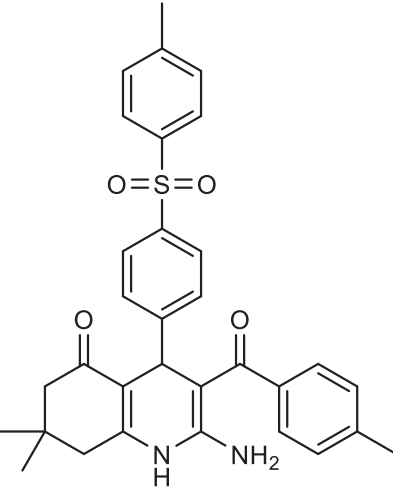
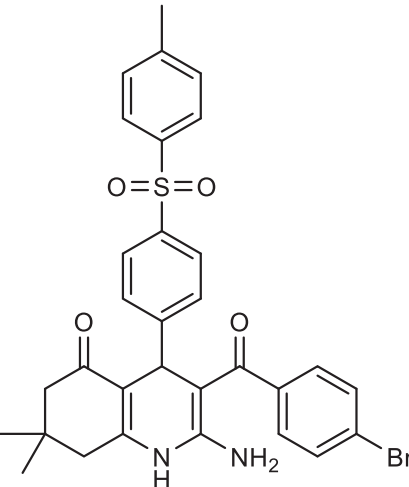
Table 1. Continued.

Compound	Conventional conditions		Ultrasound conditions	
	Time (h)	Yield %	Time (min)	Yield%
 <p><b>4d</b></p>	6	78	30	90
 <p><b>4e</b></p>	6	78	30	90
 <p><b>4f</b></p>	5	84	25	95

(continued)



Table 1. Continued.

Compound	Conventional conditions		Ultrasound conditions	
	Time (h)	Yield %	Time (min)	Yield%
 <p><b>4j</b></p>	6	79	30	92
 <p><b>4k</b></p>	6	78	30	92
 <p><b>4l</b></p>	6	78	30	90

IR (KBr)  $\nu_{\max}/\text{cm}^{-1}$ : 3213 (NH), 1714, 1688 (2C=O), 1310, 1211 (SO<sub>2</sub>); <sup>1</sup>H NMR (400 MHz, DMSO-d<sub>6</sub>):  $\delta$  0.80 (s, 3H, CH<sub>3</sub>), 0.98 (s, 3H, CH<sub>3</sub>), 1.97 (d, 1H, *J* = 16 Hz, H-8a), 2.15 (d, 1H, *J* = 16 Hz, H-8b), 2.28 (s, 3H, CH<sub>3</sub>), 2.33 (d, 1H, *J* = 16.4 Hz, H-6a), 2.41 (d, 1H, *J* = 16.4 Hz, H-6b), 3.49 (s, 3H, CH<sub>3</sub> ester), 4.91 (s, 1H, CH-4), 7.35 (d, 2H, *J* = 7.6 Hz, ArH), 7.39 (d, 2H, *J* = 7.72 Hz, ArH), 7.76–7.80 (m, 5H, ArH), 9.21 (br's, 1H, NH, D<sub>2</sub>O exchangeable). <sup>13</sup>C NMR (100 MHz, DMSO-d<sub>6</sub>):  $\delta$  18.8, 27.1, 29.3, 32.7, 36.7, 50.5, 51.3, 102.7, 109.6, 127.5, 127.8, 132.1, 138.9, 144.7, 153.4, 167.4, 194.8; MS *m/z* (%): 465 (M<sup>+</sup>, 40.9). Anal. for C<sub>26</sub>H<sub>27</sub>NO<sub>5</sub>S: C, 67.08; H, 5.85; N, 3.01; S, 6.89. found: C, 67.29; H, 5.79; N, 2.90; S, 6.83%.

#### 2.2.2.2. Ethyl 7,7-dimethyl-5-oxo-4-(4-(phenylsulfonyl)phenyl)-2-(trifluoromethyl)-1,4,5,6,7,8-hexahydroquinoline-3-carboxylate

(4b). Mp 245–247 °C. IR (KBr)  $\nu_{\max}/\text{cm}^{-1}$ : 3221 (NH), 1717, 1688 (2C=O), 1314, 1210 (SO<sub>2</sub>); <sup>1</sup>H NMR (400 MHz, DMSO-d<sub>6</sub>):  $\delta$  0.85 (s, 3H, CH<sub>3</sub>), 0.98 (s, 3H, CH<sub>3</sub>), 1.13 (t, 3H, *J* = 7 Hz CH<sub>3</sub> ester) 1.96 (d, 1H, *J* = 16 Hz, H-8a), 2.16 (d, 1H, *J* = 16 Hz, H-8b), 2.35 (d, 1H, *J* = 16.4 Hz, H-6a), 2.43 (d, 1H, *J* = 16.4 Hz, H-6a), 4.19 (q, 2H, *J* = 7 Hz, CH<sub>2</sub> Ester), 4.92 (s, 1H, CH-4), 7.35 (d, 2H, *J* = 7.6 Hz, ArH), 7.39 (d, 2H, *J* = 7.72 Hz, ArH), 7.71–7.86 (m, 5H, ArH), 9.22 (br's, 1H, NH, D<sub>2</sub>O exchangeable). <sup>13</sup>C NMR (100 MHz, DMSO-d<sub>6</sub>):  $\delta$  18.9, 27.1, 29.3, 32.7, 36.7, 51.3, 62.0, 102.6, 109.5, 123.2, 127.6, 127.7, 130.2, 134.9, 138.9, 141.7, 146.7, 150.6, 153.6, 167.4, 194.7; MS *m/z* (%): 533 (M<sup>+</sup>, 51.5). Anal. for C<sub>27</sub>H<sub>26</sub>F<sub>3</sub>NO<sub>5</sub>S: C, 60.78; H, 4.91; N, 2.63; S, 6.01. found: C, 60.99; H, 4.87; N, 2.53; S, 5.94%.

#### 2.2.2.3. Ethyl 2-amino-7,7-dimethyl-5-oxo-4-(4-(phenylsulfonyl)phenyl)-1,4,5,6,7,8-hexahydroquinoline-3-carboxylate

(4c). Mp 238–240 °C. IR (KBr)  $\nu_{\max}/\text{cm}^{-1}$ : 3389, 3282 (NH<sub>2</sub>), 3216 (NH), 1712, 1689 (2C=O), 1310, 1196 (SO<sub>2</sub>); <sup>1</sup>H NMR (400 MHz, CDCl<sub>3</sub>):  $\delta$  0.96 (s, 3H, CH<sub>3</sub>), 1.09 (s, 3H, CH<sub>3</sub>), 1.14(t, 3H, *J* = 7.2 Hz, CH<sub>3</sub> ester), 1.84 (br's, 2H, NH<sub>2</sub>, D<sub>2</sub>O exchangeable), 2.17 (dd, 2H, *J* = 14 Hz, H-8a and H8b), 2.41 (s, 2H, CH<sub>2</sub>-6), 4.03(q, 2H, *J* = 7.2 Hz, CH<sub>2</sub> ester), 4.66 (s, 1H, C4 -H), 7.15 (d, 2H, *J* = 7.6 Hz, ArH), 7.21 (d, 2H, *J* = 7.72 Hz, ArH), 7.39–7.78 (m, 5H, ArH), 9.54 (br's, 1H, NH, D<sub>2</sub>O exchangeable). <sup>13</sup>C NMR (100 MHz, CDCl<sub>3</sub>):  $\delta$  14.2, 27.4, 29.1, 32.2, 33.5, 40.7, 50.7, 59.8, 80.3, 116.4, 122.0, 126.9, 127.9, 129.6, 131.6, 136.0, 144.5, 149.5, 158.4, 161.5, 168.9, 196.4; MS *m/z* (%): 480 (M<sup>+</sup>, 28.7). Anal. for C<sub>26</sub>H<sub>28</sub>N<sub>2</sub>O<sub>5</sub>S: C, 64.98; H, 5.87; N, 5.83; S, 6.67. found: C, 65.20; H, 5.81; N, 5.75; S, 6.59%.

#### 2.2.2.4. 2-Amino-3-benzoyl-7,7-dimethyl-4-(4-(phenylsulfonyl)phenyl)-4,6,7,8-tetrahydroquinolin-5(1H)-one

(4d). Mp > 300 °C. IR (KBr)  $\nu_{\max}/\text{cm}^{-1}$ : 3339, 3291 (NH<sub>2</sub>), 3222 (NH), 1699, 1685 (2C=O), 1310, 1206 (SO<sub>2</sub>); <sup>1</sup>H NMR (850 MHz, CDCl<sub>3</sub>):  $\delta$  0.96 (s, 3H, CH<sub>3</sub>), 1.09 (s, 3H, CH<sub>3</sub>), 2.18 (dd, 2H, *J* = 14 Hz, H-8a and H-8b), 2.42 (dd, 2H, *J* = 16.9 Hz, H-6a and H-6b), 4.65 (s, 1H, CH-4), 6.21 (br's, 2H, NH<sub>2</sub>, D<sub>2</sub>O exchangeable), 6.82 (d, 2H, *J* = 7.4 Hz, ArH), 7.14 (d, 2H, *J* = 7.6 Hz, ArH), 7.33 (d, 2H, *J* = 7.1 Hz, ArH), 7.56–7.81 (m, 4H, ArH), 8.11–8.48 (m, 4H, ArH), 9.31 (br's, 1H, NH, D<sub>2</sub>O exchangeable). <sup>13</sup>C NMR (213 MHz, CDCl<sub>3</sub>):  $\delta$  27.3, 29.1, 32.3, 33.4, 40.6, 50.7, 80.2, 50.5, 51.3, 116.3, 126.2, 127.4, 128.1, 129.7, 129.9, 130.1, 130.8, 134.2, 137.3, 144.9, 145.1, 158.3, 168.9, 190.7, 196.5; MS *m/z* (%): 512 (M<sup>+</sup>, 39.1). Anal. for C<sub>30</sub>H<sub>28</sub>N<sub>2</sub>O<sub>4</sub>S: C, 70.29; H, 5.51; N, 5.46; S, 6.25. found: C, 70.52; H, 5.47; N, 5.36; S, 6.17%.

#### 2.2.2.5. 2-Amino-7,7-dimethyl-3-(4-methylbenzoyl)-4-(4-(phenylsulfonyl)phenyl)-4,6,7,8-tetrahydroquinolin-5(1H)-one

(4e). Mp > 300 °C. IR (KBr)  $\nu_{\max}/\text{cm}^{-1}$ : 3331, 3291 (NH<sub>2</sub>), 3226 (NH), 1691, 1683 (2C=O), 1314, 1201(SO<sub>2</sub>); <sup>1</sup>H NMR (850 MHz, CDCl<sub>3</sub>):  $\delta$  0.96 (s, 3H, CH<sub>3</sub>), 1.09 (s, 3H, CH<sub>3</sub>), 2.17 (dd, 2H, *J* = 16.15 Hz, H-8a and

H-8b), 2.41 (dd, 2H, *J* = 17.83 Hz, H-6a and H-6b), 2.58 (s, 3H, CH<sub>3</sub>), 4.69 (s, 1H, C4 -H), 6.26 (br's, 2H, NH<sub>2</sub>, D<sub>2</sub>O exchangeable), 6.87 (d, 2H, *J* = 8.5 Hz), 6.88 – 6.89 (m, 5H, ArH), 7.20–7.23 (m, 4H, Ar H), 7.27 (d, 2H, *J* = 8.4 Hz, ArH), 9.05 (br's, 1H, NH, D<sub>2</sub>O exchangeable). <sup>13</sup>C NMR (213 MHz, CDCl<sub>3</sub>):  $\delta$  18.2, 27.3, 29.1, 32.2, 33.2, 40.6, 50.7, 80.5, 116.6, 128.8, 129.6, 129.9, 131.2, 133.6, 137.4, 139.2, 141.6, 158.3, 169.0, 189.9, 196.5; MS *m/z* (%): 526 (M<sup>+</sup>, 74.3). Anal. for C<sub>31</sub>H<sub>30</sub>N<sub>2</sub>O<sub>4</sub>S: C, 70.70; H, 5.74; N, 5.32; S, 6.09. found: C, 70.88; H, 5.71; N, 5.24; S, 6.04%.

#### 2.2.2.6. 2-Amino-3-(4-bromobenzoyl)-7,7-dimethyl-4-(4-(phenylsulfonyl)phenyl)-4,6,7,8-tetrahydroquinolin-5(1H)-one

(4f). Mp > 300 °C. IR (KBr)  $\nu_{\max}/\text{cm}^{-1}$ : 3310, 3296 (NH<sub>2</sub>), 3221 (NH), 1691, 1682 (2C=O), 1305, 1193 (SO<sub>2</sub>); <sup>1</sup>H NMR (850 MHz, DMSO-d<sub>6</sub>):  $\delta$  0.96 (s, 3H, CH<sub>3</sub>), 1.04 (s, 3H, CH<sub>3</sub>), 2.13 (dd, 2H, *J* = 16.00 Hz, H-8a and H-8b), 2.42 (dd, 2H, *J* = 16.4 Hz, H-6a and H-6b), 4.62 (s, 1H, C4 -H), 6.23 (br's, 2H, NH<sub>2</sub>, D<sub>2</sub>O exchangeable), 6.91 – 7.16 (m, 7H, ArH), 7.33–7.52 (m, 4H, Ar H), 7.65 (d, 2H, *J* = 8.2 Hz, ArH), 9.11 (br's, 1H, NH, D<sub>2</sub>O exchangeable). <sup>13</sup>C NMR (213 MHz, CDCl<sub>3</sub>):  $\delta$  27.3, 29.1, 32.2, 33.2, 40.6, 50.7, 80.5, 116.6, 128.8, 129.6, 129.9, 131.2, 133.6, 137.4, 139.2, 141.6, 158.3, 169.0, 189.9, 196.5; MS *m/z* (%): 591 (M<sup>+</sup>, 77.1), 593 (M<sup>+</sup>+2, 76.8). Anal. for C<sub>30</sub>H<sub>27</sub>BrN<sub>2</sub>O<sub>4</sub>S: C, 60.92; H, 4.60; N, 4.74; S, 5.42. found: C, 61.11; H, 4.55; N, 4.65; S, 5.37%.

#### 2.2.2.7. Methyl 2,7,7-trimethyl-5-oxo-4-(4-tosylphenyl)-1,4,5,6,7,8-hexahydroquinoline-3-carboxylate

(4g). Mp 236–238 °C. IR (KBr)  $\nu_{\max}/\text{cm}^{-1}$ : 3218 (NH), 1723, 1674 (2C=O), 1312, 1206 (SO<sub>2</sub>); <sup>1</sup>H NMR (850 MHz, CDCl<sub>3</sub>):  $\delta$  0.91 (s, 3H, CH<sub>3</sub>), 1.01 (s, 3H, CH<sub>3</sub>), 2.02 (d, 1H, *J* = 16 Hz, H-8a), 2.09 (d, 1H, *J* = 16 Hz, H-8b), 2.33 (s, 3H, CH<sub>3</sub>), 2.34 (s, 3H, CH<sub>3</sub>), 2.36 (s, 2H, CH<sub>2</sub>-6), 4.42 (s, 1H, C4 -H), 3.16 (s, 3H, CH<sub>3</sub> ester), 4.41 (s, 1H, CH-4), 6.70 (d, 2H, *J* = 7.6 Hz, ArH), 6.87 (d, 2H, *J* = 7.8 Hz, ArH), 7.56–7.81 (m, 4H, ArH), 9.12 (br's, 1H, NH, D<sub>2</sub>O exchangeable). <sup>13</sup>C NMR (213 MHz, CDCl<sub>3</sub>):  $\delta$  19.2, 21.3, 27.3, 28.3, 32.2, 39.5, 40.8, 49.7, 50.2, 104.2, 117.6, 128.8, 129.4, 134.1, 136.1, 153.6, 154.2, 156.1, 164.3, 197.6; MS *m/z* (%): 479 (M<sup>+</sup>, 49). Anal. for C<sub>27</sub>H<sub>29</sub>NO<sub>5</sub>S: C, 67.62; H, 6.10; N, 2.92; S, 6.68. found: C, 67.80; H, 6.06; N, 2.83; S, 6.63%.

#### 2.2.2.8. Ethyl 7,7-dimethyl-5-oxo-4-(4-tosylphenyl)-2-(trifluoromethyl)-1,4,5,6,7,8-hexahydroquinoline-3-carboxylate

(4h). Mp 241–243 °C. IR (KBr)  $\nu_{\max}/\text{cm}^{-1}$ : 3231(NH), 1726, 1684 (2C=O), 1303, 1215 (SO<sub>2</sub>); <sup>1</sup>H NMR (400 MHz, DMSO-d<sub>6</sub>):  $\delta$  0.89 (s, 3H, CH<sub>3</sub>), 1.01 (s, 3H, CH<sub>3</sub>), 1.16 (t, 3H, *J* = 7 Hz CH<sub>3</sub> ester), 2.01 (d, 1H, *J* = 16 Hz, H-8a), 2.14 (d, 1H, *J* = 16 Hz, H-8b), 2.33 (d, 1H, *J* = 16.4 Hz, H-6a), 2.43 (d, 1H, *J* = 16.4 Hz, H-6b), 2.48 (s, 3H, CH<sub>3</sub>), 4.12 (q, 2H, *J* = 7 Hz, CH<sub>2</sub> Ester), 4.91 (s, 1H, CH-4), 7.31 (d, 2H, *J* = 7.00 Hz, ArH), 7.41–7.56 (m, 4H, ArH), 7.58 (d, 2H, *J* = 7.72 Hz, ArH), 9.26 (br's, 1H, NH, D<sub>2</sub>O exchangeable). <sup>13</sup>C NMR (100 MHz, DMSO-d<sub>6</sub>):  $\delta$  14.3, 18.2, 27.3, 29.1, 32.5, 37.2, 43.6, 51.1, 62.0, 100.4, 113.5, 124.2, 128.6, 129.2, 129.8, 130.2, 136.7, 138.2, 141.8, 146.7, 150.6, 153.6, 168.6, 194.8; MS *m/z* (%): 547 (M<sup>+</sup>, 39). Anal. for C<sub>28</sub>H<sub>28</sub>F<sub>3</sub>NO<sub>5</sub>S: C, 61.42; H, 5.15; N, 2.56; S, 5.85. found: C, 61.63; H, 5.09; N, 2.46; S, 5.79%.

#### 2.2.2.9. Ethyl 2-amino-7,7-dimethyl-5-oxo-4-(4-tosylphenyl)-1,4,5,6,7,8-hexahydroquinoline-3-carboxylate

(4i). Mp 281–283 °C. IR (KBr)  $\nu_{\max}/\text{cm}^{-1}$ : 3394, 3286 (NH<sub>2</sub>), 3231(NH), 1726, 1684 (2C=O), 1303, 1215 (SO<sub>2</sub>); <sup>1</sup>H NMR (400 MHz, DMSO-d<sub>6</sub>):  $\delta$  0.92 (s, 3H, CH<sub>3</sub>), 0.99 (s, 3H, CH<sub>3</sub>), 1.12(t, 3H, *J* = 7.2 Hz, CH<sub>3</sub> ester), 1.89 (br's, 2H, NH<sub>2</sub>, D<sub>2</sub>O exchangeable), 2.11 (dd, 2H, *J* = 14 Hz, H-8a and H8b), 2.36 (s, 2H, CH<sub>2</sub>-6), 2.44 (s, 3H, CH<sub>3</sub>), 4.11(q, 2H, *J* = 7.2 Hz, CH<sub>2</sub> ester), 4.71 (s, 1H, C4

–H), 7.15 (d, 2H,  $J=7.2$  Hz, ArH), 7.21 (d, 2H,  $J=7.6$  Hz, ArH), 7.36–7.52 (m, 5H, ArH), 9.21 (br's, 1H, NH, D<sub>2</sub>O exchangeable). <sup>13</sup>C NMR (100 MHz, CDCl<sub>3</sub>):  $\delta$  14.3, 18.9, 27.3, 29.6, 32.4, 35.2, 41.7, 52.4, 59.6, 83.1, 117.7, 127.6, 127.7, 129.7, 130.6, 133.9, 136.3, 138.3, 145.5, 149.5, 161.9, 168.7, 194.5; OMS  $m/z$  (%): 494 (M<sup>+</sup>, 62.9), Anal. for C<sub>27</sub>H<sub>30</sub>N<sub>2</sub>O<sub>5</sub>S: C, 65.57; H, 6.11; N, 5.66; S, 6.48. found: C, 65.74; H, 6.06; N, 2.39; S, 6.41%.

**2.2.2.10. 2-Amino-3-benzoyl-7,7-dimethyl-4-(4-tosylphenyl)-4,6,7,8-tetrahydroquinolin-5(1H)-one (4j).** Mp > 300 °C. IR (KBr)  $\nu_{\max}/\text{cm}^{-1}$ : 3382, 3267(NH<sub>2</sub>), 3211(NH), 1691, 1681 (2C=O), 1310, 1211 (SO<sub>2</sub>); <sup>1</sup>H NMR (850 MHz, CDCl<sub>3</sub>):  $\delta$  0.94 (s, 3H, CH<sub>3</sub>), 1.01 (s, 3H, CH<sub>3</sub>), 2.22 (dd, 2H,  $J=14$  Hz, H-8a and H-8b), 2.31 (dd, 2H,  $J=16.9$  Hz, H-6a and H-6b), 2.38 (s, 3H, CH<sub>3</sub>), 4.52 (s, 1H, CH-4), 6.28 (br's, 2H, NH<sub>2</sub>, D<sub>2</sub>O exchangeable), 6.79 (d, 2H,  $J=7.8$  Hz, ArH), 7.32 (d, 2H,  $J=7.4$  Hz, ArH), 7.46–7.71 (m, 4H, ArH), 7.77–8.01 (m, 4H, ArH), 9.31 (br's, 1H, NH, D<sub>2</sub>O exchangeable). <sup>13</sup>C NMR (213 MHz, CDCl<sub>3</sub>):  $\delta$  18.23, 27.3, 29.2, 32.4, 34.2, 40.8, 50.1, 81.3, 50.5, 51.3, 116.3, 126.2, 127.4, 128.1, 129.7, 129.9, 130.1, 130.8, 134.2, 137.3, 144.9, 145.1, 158.3, 168.9, 190.7, 196.5; MS  $m/z$  (%): 526 (M<sup>+</sup>, 41.3), Anal. for C<sub>31</sub>H<sub>30</sub>N<sub>2</sub>O<sub>4</sub>S: C, 70.70; H, 5.74; N, 5.32; S, 6.09. found: C, 70.87; H, 5.69; N, 5.25; S, 6.02%.

**2.2.2.11. 2-Amino-7,7-dimethyl-3-(4-methylbenzoyl)-4-(4-tosylphenyl)-4,6,7,8-tetrahydroquinolin-5(1H)-one (4k).** Mp > 300 °C. IR (KBr)  $\nu_{\max}/\text{cm}^{-1}$ : 3379, 3229(NH<sub>2</sub>), 3211(NH), 1690, 1676 (2C=O), 1310, 1196 (SO<sub>2</sub>); <sup>1</sup>H NMR (850 MHz, CDCl<sub>3</sub>):  $\delta$  0.93 (s, 3H, CH<sub>3</sub>), 0.97 (s, 3H, CH<sub>3</sub>), 2.01 (dd, 2H,  $J=16$  Hz, H-8a and H-8b), 2.22 (dd, 2H,  $J=16.2$  Hz, H-6a and H-6b), 2.36 (s, 3H, CH<sub>3</sub>), 2.39 (s, 3H, CH<sub>3</sub>), 4.61 (s, 1H, C4 –H), 6.01 (br's, 2H, NH<sub>2</sub>, D<sub>2</sub>O exchangeable), 7.22–7.41 (m, 4H, ArH), 7.49(d, 2H,  $J=7.2$  Hz, ArH), 7.56–7.67 (m, 4H, ArH), 7.77 (d, 2H,  $J=7.8$  Hz, ArH), 9.23 (br's, 1H, NH, D<sub>2</sub>O exchangeable). <sup>13</sup>C NMR (213 MHz, CDCl<sub>3</sub>):  $\delta$  18.7, 19.1, 27.2, 29.4, 32.8, 37.1, 39.9, 51.1, 80.3, 116.5, 128.5, 128.8, 129.5, 129.7, 130.3, 130.9, 132.1, 138.3, 138.9, 139.0, 144.1, 152.5, 156.1, 168.9, 189.2, 195.6; MS  $m/z$  (%): 540 (M<sup>+</sup>, 65.1), Anal. for C<sub>32</sub>H<sub>32</sub>N<sub>2</sub>O<sub>4</sub>S: C, 71.09; H, 5.97; N, 5.18; S, 5.93. found: C, 71.29; H, 5.93; N, 5.08; S, 5.87%.

**2.2.2.12. 2-Amino-3-(4-bromobenzoyl)-7,7-dimethyl-4-(4-tosylphenyl)-4,6,7,8-tetrahydroquinolin-5(1H)-one (4l).** Mp > 300 °C. IR (KBr)  $\nu_{\max}/\text{cm}^{-1}$ : 3379, 3229(NH<sub>2</sub>), 3211(NH), 1690, 1676 (2C=O), 1310, 1196 (SO<sub>2</sub>); <sup>1</sup>H NMR (850 MHz, DMSO-d<sub>6</sub>):  $\delta$  0.93 (s, 3H, CH<sub>3</sub>), 1.01 (s, 3H, CH<sub>3</sub>), 2.11 (dd, 2H,  $J=16.00$  Hz, H-8a and H-8b), 2.31 (dd, 2H,  $J=16.4$  Hz, H-6a and H-6b), 2.39 (s, 3H, CH<sub>3</sub>), 4.45 (s, 1H, C4 –H), 6.41 (br's, 2H, NH<sub>2</sub>, D<sub>2</sub>O exchangeable), 7.21–7.46 (m, 8H, ArH), 7.53–7.74 (m, 2H, Ar H), 7.85 (d, 2H,  $J=7.8$  Hz, ArH), 9.29 (br's, 1H, NH, D<sub>2</sub>O exchangeable). <sup>13</sup>C NMR (213 MHz, CDCl<sub>3</sub>):  $\delta$  19.2, 27.1, 29.6, 32.4, 36.2, 40.1, 50.7, 80.9, 115.1, 127.9, 128.3, 129.8, 129.9, 131.6, 133.4, 138.6, 140.0, 148.6, 151.1, 168.4, 190.3, 196.8; MS  $m/z$  (%): 605 (M<sup>+</sup>, 29.6), 607 (M<sup>+</sup>+2, 29.5). Anal. for C<sub>32</sub>H<sub>29</sub>BrN<sub>2</sub>O<sub>4</sub>S: C, 61.49; H, 4.83; N, 4.63; S, 5.29. found: C, 61.68; H, 4.79; N, 4.55; S, 5.25%.

### 2.3. Biological evaluation

#### 2.3.1. In vitro cytotoxicity

MTT assay was used to evaluate the *in vitro* cytotoxicity of the new compounds against breast cancer cell lines MCF-7<sup>38</sup>. More details are present in the Supplementary file.

#### 2.3.2. Kinase assays

The activities of the examined compounds against EGFR, HER2, PDGFR-b, and VEGFR2 were *in vitro* tested using Abcam's Human In cell ELISA Kit (ab 126419) for EGFR, ADP-Glo™ Kinase Assay for Her2, PDGFR-b, Active, Recombinant protein expressed in Sf9 cells for VEGFR2 (KDR) Kinase Assay Kit Catalog #40325, respectively. The procedure of the used kits was done according to the manufacturer, s instructions.

#### 2.3.3. Cell cycle analysis and apoptosis detection

Cell cycle analysis and apoptosis investigation were carried out by flow cytometry.<sup>39,40</sup> MCF-7 cells were seeded at  $8 \times 10^4$  and incubated at 37 °C, 5% CO<sub>2</sub> overnight. After treatment with the tested compound, for 24 h, cell pellets were collected and centrifuged (300 g, 5 min).

### 2.4. Molecular docking method

The docking studies had been calculated and studies using Molecular Operating Environment (MOE, 2019.0102) software<sup>41–43</sup>. All minimisations were performed with MOE until an RMSD gradient of 0.1 kcal·mol<sup>-1</sup> Å<sup>-1</sup> with MMFF94x force field and the partial charges were automatically calculated.

#### 2.4.1. Human epidermal growth factor receptor 2 (HER2)

The X-ray crystallographic structure of human HER2 (HER2) co-crystalised with 2-{2-[4-({5-chloro-6-[3-(trifluoromethyl)phenoxy]pyridin-3-yl}amino)-5H-pyrrolo[3,2-d]pyrimidin-5-yl]ethoxy}ethanol (03Q) (PDB ID: 3PP0) was downloaded from the protein data bank (<https://www.rcsb.org/structure/3PP0>). For each co-crystalised enzyme, water molecules and ligands which are not involved in the binding were removed. The protein was prepared for the docking study using *Protonate 3D* protocol in MOE with default options. The co-crystalised ligand (03Q) was used to define the binding site for docking. Triangle Matcher placement method and London dG scoring function were used for docking.

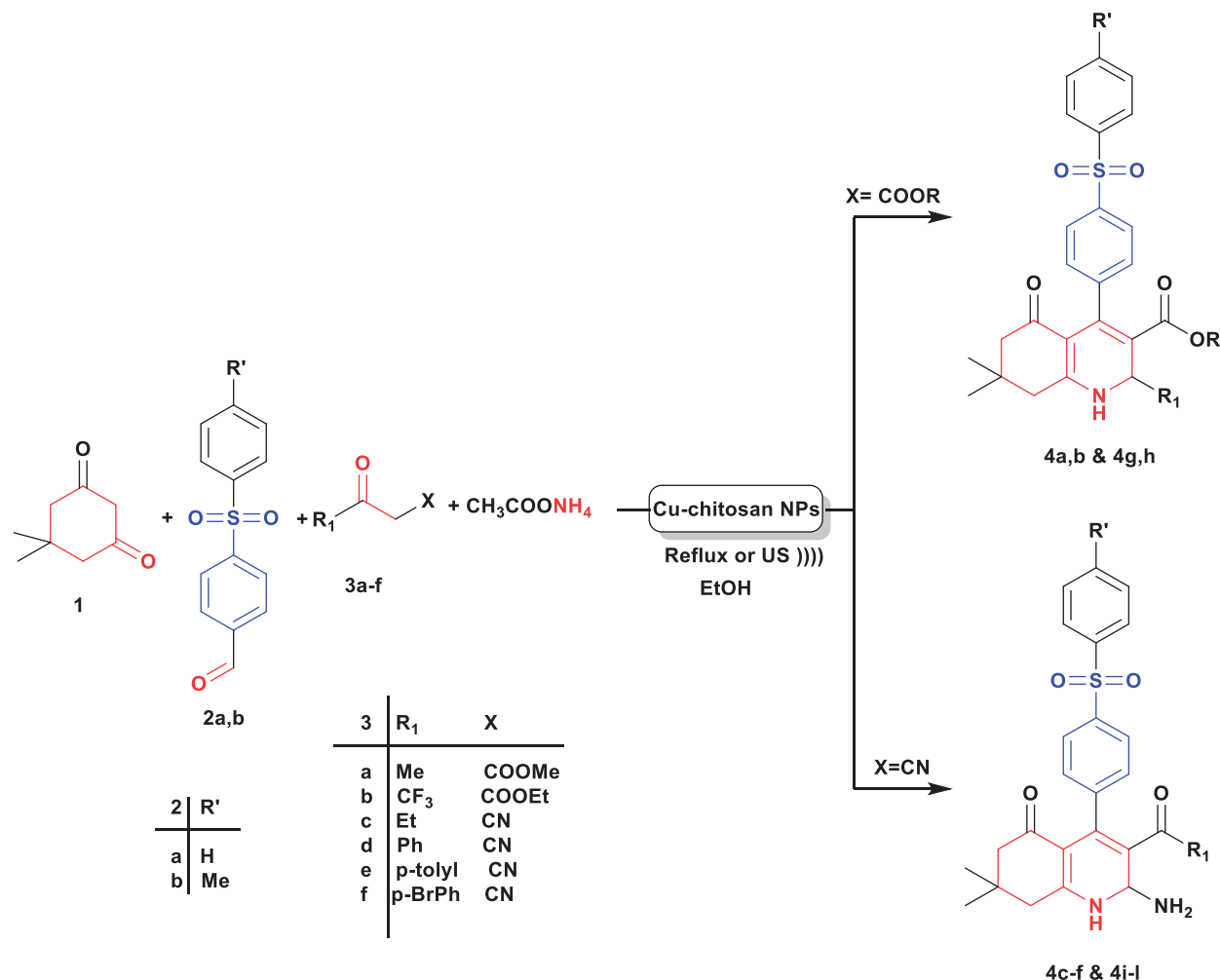
#### 2.4.2. Platelet-derived growth factor receptor $\alpha$ (PDGFRA)

The X-ray crystallographic structure of human platelet-derived growth factor receptor  $\alpha$  (PDGFRA) co-crystalised with Imatinib (PDB ID: 6JOL) was downloaded from the protein data bank (<https://www.rcsb.org/structure/6JOL>). For each co-crystalised enzyme, water molecules and ligands which are not involved in the binding were removed. The protein was prepared for the docking study using *Protonate 3D* protocol in MOE with default options. The co-crystalised ligand (imatinib) was used to define the binding site for docking. Triangle Matcher placement method and London dG scoring function were used for docking.

## 3. Results and discussion

### 3.1. Chemistry

We synthesised a series of 12 compounds bearing 4,6,7,8-tetrahydroquinolin-5(1H)-one scaffold according to Scheme 1. Compounds **4a–l** were synthesised following the previously reported optimised multicomponent green reaction procedures<sup>35</sup> by treating dimedone (**1**) and aldehydes **2a, b** namely; 4-(phenylsulfonyl)benzaldehyde and 4-tosylbenzaldehyde respectively with various active methylene compounds **3a–f** in the presence of ammonium acetate in ethanol



**Scheme 1.** Synthesis of novel tetrahydroquinolin-5(1H)-ones **4a-l**.

under ultrasonic irradiation conditions using chitosan decorated copper nanoparticles (CS/CuNPs) as a catalyst.

The progress of reactions was monitored by TLC till the disappearance of reactants. The beneficial effect of ultrasound is noticeable over conventional conditions on this reaction (Table 1), reducing the reaction time from 5 to 6 h into 20–30 min. and the yield of reaction increased to 90–95% under ultrasound irradiation compared to 78–84% under conventional conditions (Table 1).

The reaction products were identified as the polysubstituted 4,6,7,8-tetrahydroquinolin-5(1H)-ones **4a-l** in all cases based on its <sup>1</sup>H-NMR spectrum. For example, the <sup>1</sup>H-NMR spectrum of the isolated reaction product **4a** revealed five singlet signals at δ 0.80, 0.98, 2.28, 3.49, and 4.91 ppm due to the four methyl groups and CH-4, respectively, two shielded doublets (dd) at δ 1.97, 2.15, ppm with coupling constants of approximately 16 Hz due to the H8a, H8b, another two shielded doublets (dd) at δ 2.33, and 2.41 ppm with coupling constant of 16.4 Hz due to H6a, H6b and two doublets and aromatic multiplet in the region 7.76–7.80 ppm due to 9 aromatic protons. In addition to a D<sub>2</sub>O exchangeable signal at 9.21 indicates the presence of NH group. Also, the <sup>13</sup>C-NMR of the isolated product **4a** adds strong evidence for the proposed structure, which agrees with the structure formed as shown in Scheme 1 (cf. experimental part).

The apparent effect of ultrasound on the reaction mentioned above may be attributed to the fact that ultrasonic irradiation gives the reactants sufficient energy to exceed the energy barrier of the

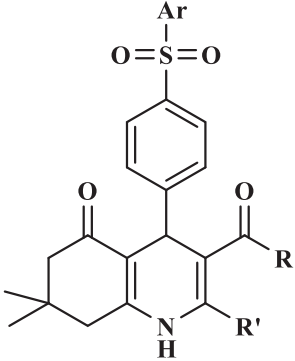
reaction, thus, 4,6,7,8-tetrahydroquinolin-5(1H)-ones **4a-l** formed. This sufficient energy can be reasonably interpreted in terms of the physical phenomenon called acoustic cavitation (in our case, at solid-liquid interfaces). The most accepted proposed mechanism for the effect of cavitation near surfaces<sup>44,45</sup> is microjet impact and shockwave damage. Along with the shock wave associated with the cavitation collapse, the jet causes localised deformation and surface erosion, which increases the possible reaction area. Therefore, the treated surfaces contain an increased number of dislocations that are widely considered to be the active sites in catalysis.

### 3.2. Biological evaluation

#### 3.2.1. In vitro anticancer activity

This work represents the construction of a new series of compounds bearing 7,7-dimethyl-4-(4-(phenylsulfonyl)phenyl)-4,6,7,8-tetrahydroquinolin-5(1H)-one scaffold **4a-l** of potential anti-breast cancer activity. To evaluate the cytotoxic activity of the new derivatives, they were subjected to MTT cell viability assay against human breast cancer MCF-7 cell line utilising staurosporine as a reference drug.<sup>46–48</sup> The obtained data were represented as IC<sub>50</sub> (μM) values which are the average of at least three independent experiments and tabulated in Table 2.

The new derivatives showed variable degrees of cytotoxic activities. Interestingly, the 2-trifluoromethyl derivative **4b** exhibited about 2.5-fold more potent activity than the standard drug

**Table 2.** *In vitro* cell cytotoxic activity of the new compounds against MCF-7 cancer cells.


Compound No		Anticancer activity against MCF-7 cells IC <sub>50</sub> (μM) mean ± SD
4a	Ar = phenyl; R = OCH <sub>3</sub> ; R' = CH <sub>3</sub>	0.103 ± 0.013
4b	Ar = phenyl; R = OC <sub>2</sub> H <sub>5</sub> ; R' = CF <sub>3</sub>	0.002 ± 0.001
4c	Ar = phenyl; R = OC <sub>2</sub> H <sub>5</sub> ; R' = NH <sub>2</sub>	0.015 ± 0.002
4d	Ar, R = phenyl; R' = NH <sub>2</sub>	0.007 ± 0.001
4e	Ar, R = <i>p</i> -tolyl; R' = NH <sub>2</sub>	0.004 ± 0.002
4f	Ar = phenyl; R = <i>p</i> -Br-phenyl; R' = NH <sub>2</sub>	0.027 ± 0.014
4g	Ar = <i>p</i> -tolyl; R = OCH <sub>3</sub> ; R' = CH <sub>3</sub>	0.027 ± 0.003
4h	Ar = <i>p</i> -tolyl; R = OC <sub>2</sub> H <sub>5</sub> ; R' = CF <sub>3</sub>	0.041 ± 0.006
4i	Ar = <i>p</i> -tolyl; R = OC <sub>2</sub> H <sub>5</sub> ; R' = NH <sub>2</sub>	0.023 ± 0.003
4j	Ar = <i>p</i> -tolyl; R = phenyl; R' = NH <sub>2</sub>	0.003 ± 0.005
4k	Ar, R = <i>p</i> -tolyl; R' = NH <sub>2</sub>	0.004 ± 0.001
4l	Ar = <i>p</i> -tolyl; R = <i>p</i> -Br-phenyl; R' = NH <sub>2</sub>	0.007 ± 0.001
Staurosporine		0.005 ± 0.002

**Table 3.** The effect of some compounds as representative examples against the normal WI38 cells.

Compound No.	IC <sub>50</sub> (μM) mean ± SD
4e	0.0149 ± 0.003
4j	0.048 ± 0.008
4b	0.045 ± 0.013
4k	0.0176 ± 0.009
Staurosporine	0.013 ± 0.002

staurosporine (IC<sub>50</sub>; 0.002 μM, IC<sub>50</sub>staurosporine; 0.005 μM). The potent cytotoxic effect of **4b** could be explained due to the electron-withdrawing power of fluorine atom, alongside the increased carbon-fluorine bond energy, that significantly potentiates the metabolic stability of the host molecule and enhances its lipophilicity facilitating the cell membrane permeation and its pronounced cytotoxic effect<sup>38</sup>. A slight decrease in the potency was detected upon replacement of -CF<sub>3</sub> group by NH<sub>2</sub> as compounds **4j**, **4e**, **4k** exhibiting about 1–1.6-fold more potent activity than that resulted by staurosporine of IC<sub>50</sub> values of 0.003, 0.004, and 0.004 μM, respectively. Further decrease in the inhibitory activity to be 1.4-fold less potent than the standard drug was obtained upon replacement of the 3-methoxy/ethoxy groups by phenyl or *p*-bromophenyl groups as compounds **4d**, **4l**, of IC<sub>50</sub>; 0.007 μM. The rest of the compounds produced a detectable decrease in the cytotoxic potency of IC<sub>50</sub>, ranging from 0.023 to 0.103 μM. It could be noted that the significant increase in the hydrophobicity of the compounds negatively affects the cytotoxic activity of the new tetrahydroquinolinone derivatives.

### 3.2.2. The effect of compounds 4b, 4j, 4k, and 4e against the normal WI38 cells

One of the characteristics differentiating different anticancer agents from each other is the recurrence and severity of their side effects to the normal cells at their therapeutic doses. Accordingly,

**Table 4.** Protein kinase inhibition of compounds **4b** and **4j** in comparison with Sorafenib.

Compound No	EGFR	HER-2	PDGFR-α	VEGFR-2
	IC <sub>50</sub> μM × 10 <sup>-3</sup>			
<b>4b</b>	0.11 ± 0.03	0.30 ± 0.05	0.21 ± 0.04	1.05 ± 0.02
<b>4j</b>	0.07 ± 0.02	0.17 ± 0.02	0.07 ± 0.01	0.30 ± 0.06
Sorafenib	0.04 ± 0.02	0.28 ± 0.04	0.13 ± 0.02	0.17 ± 0.02

the safety profile of the most promising candidates (**4b**, **4j**, **4k**, and **4e**) was evaluated against the normal WI38 cells derived from lung tissues in comparison with staurosporine as a reference drug-using MTT assay<sup>46–48</sup> (Table 3). It is worthy of mentioning that the IC<sub>50</sub> values of the target compounds **4j**, **4b** against the normal WI38 cells were 20 and 24-fold higher than their IC<sub>50</sub> doses against the cancer cells and about 3-fold higher than the IC<sub>50</sub> value of reference drug staurosporine confirming the promising safety profile of both compounds. Whereas, less safety profile was investigated by compounds **4e** and **4k** producing IC<sub>50</sub> values against WI38 cells that were only 4-fold higher than their IC<sub>50</sub> doses against MCF-7 cells and approximately equal to that obtained by staurosporine (Table 2).

### 3.2.3. In vitro kinase inhibition assay

To explore the mechanistic insight into the cytotoxic potentials of the new quinolone compounds, *in vitro* kinase assay was performed to evaluate the kinase suppression activity of the most promising cytotoxic candidates **4b**, **4j** against four different RTK. Which are: EGFR, human epidermal growth factor receptor (HER2), PDGFR-α, and VEGFR-2. It has been detected that compound **4j** was more potent than **4b** as EGFR inhibitor with IC<sub>50</sub> values of 0.07 × 10<sup>-3</sup> and 0.11 × 10<sup>-3</sup> μM, respectively, but both were less potent than the Sorafenib of IC<sub>50</sub> 0.04 × 10<sup>-3</sup> μM (Table 4). On the

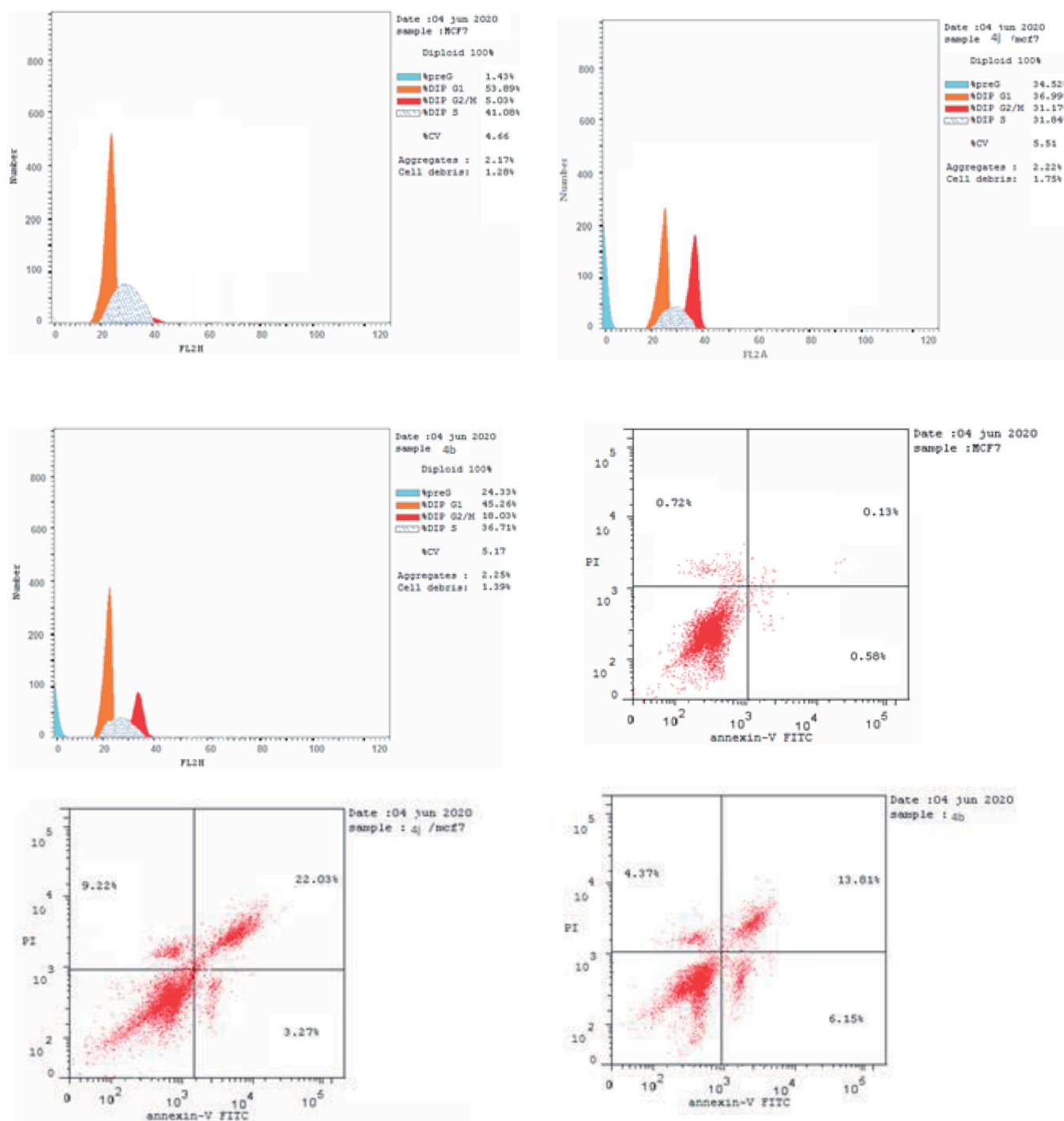


Figure 4. Apoptotic effects of compounds **4b** and **4j** against MCF-7 cells.

other hand, compound **4j** exhibited a significant inhibitory effect against HER-2, which is about 1.6 folds more potent than the Sorafenib of  $IC_{50}$ :  $0.17 \times 10^{-3} \mu\text{M}$ ,  $IC_{50\text{Sorafenib}}$ :  $0.28 \times 10^{-3} \mu\text{M}$ . Also, compound **4j** notably inhibited PDGFR- $\alpha$  by 1.9-fold more than the reference sorafenib of  $IC_{50}$ :  $0.07 \times 10^{-3}$ ,  $0.13 \times 10^{-3} \mu\text{M}$ , respectively. Furthermore, both compounds **4b** and **4j** revealed VEGFR-2 inhibitory effect of about 6.2 and 1.8-fold less than that of Sorafenib of  $IC_{50}$  values 1.05,  $0.30 \times 10^{-3} \mu\text{M}$ ,  $IC_{50\text{Sorafenib}}$ :  $0.17 \times 10^{-3} \mu\text{M}$ , respectively. Furthermore, the obtained data revealed the distinct inhibitory profile of the amino tetrahydroquinoline derivative **4j** in comparison with the reference drug sorafenib as illustrated in Table 3.

### 3.2.4. Apoptosis assay

The derivatives **4b** and **4j** were selected to study their apoptotic effects on MCF-7 cancer cells using Annexin-V/PI binding assay based on their promising cytotoxic potency and various kinase inhibitory effects. Staining MCF-7 cells was carried out with the two dyes; Annexin V/propidium iodide (PI) after treating them with compounds **4b** and **4j** at their  $IC_{50}$  concentrations of 0.002 and  $0.003 \mu\text{M}$  for 24 h. Flow cytometry method<sup>39,49</sup> has been used to detect the corresponding red (PI) and green (FITC) fluorescence. It has been noted that there was an increment in the percentages of the late apoptosis produced by the evaluated compounds **4b** and **4j** from 0.13% (control DMSO/MCF-7 cells) to 13.81% and

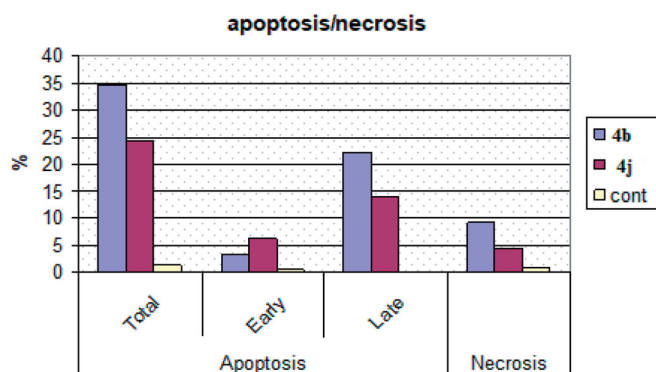


Figure 5. Apoptosis induction against MCF-7 cells caused by the derivatives **4b**, **4j**.

Table 5. Cell cycle analysis of compounds **4b** and **4j**.

Compound No	%G0-G1	%S	%G2/M	%Pre-G1
<b>4b</b>	45.26	36.71	18.03	24.33
<b>4j</b>	36.99	31.84	31.17	34.52
Cont. MCF-7	53.89	41.08	5.03	1.43

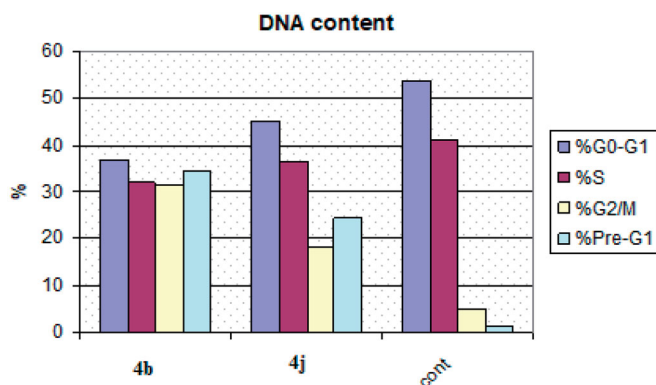


Figure 6. Cell Cycle analysis results of compounds **4b** and **4j**.

22.03%, respectively. Also, the tested compounds produced early apoptotic effects of 6.15% and 3.27% compared to 0.58% of the untreated MCF-7 cell with necrosis percent of 4.37% and 9.22%, respectively, vs. 0.66% produced by the DMSO control (Figures 4 and 5).

The proportion of the late apoptosis produced by both **4b** and **4j** was higher than the proportion of the early phase, which makes recovering the dead cells to safe ones is more challenging.

### 3.2.5. Cell cycle analysis

The induction of apoptosis is one of the most crucial tools that confirm the effectiveness of cancer therapy<sup>50</sup>. Cell cycle checkpoints are G1 (restriction or start), S (metaphase), and G2/M. One of the main functions of the anticancer therapeutics is stoppage of the cell division at these checkpoints.<sup>51</sup> Thus, MCF-7 cells were incubated with compounds **4b** and **4j** at their IC<sub>50</sub> concentrations (0.002, 0.003 μM) for 24 h. The cells were stained with Annexin V/PI and examined using flow cytometry procedure. The resultant data revealed that there was cell accumulation of percentages 24.33% and 18.03% at pre G1 and G2/M phases in MCF-7 cells treated with compound **4b** and cell accumulation percentages of 34.52% and 31.17% at pre G1 and G2/M phases in MCF-7 cells treated with compound **4j** comparing to 1.43% and 5.03% of the untreated MCF-7 cells. This result represents that there was cell

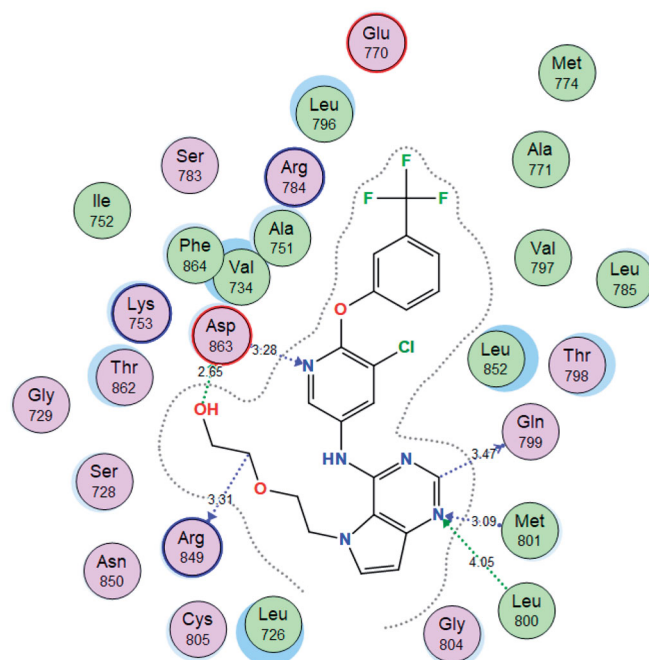


Figure 7. 2D interactions of 03Q within HER2 active site.

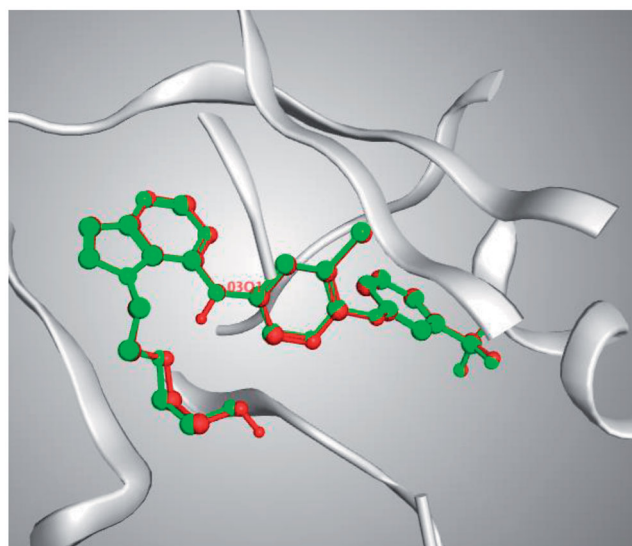


Figure 8. 3D representation of the superimposition of the co-crystallised (red) and the docking pose (green) of 30Q in the active site of HER2.

cycle arrest at G2/M phase with mitotic cycle cessation (Table 5, Figure 6).

## 4. Molecular docking study

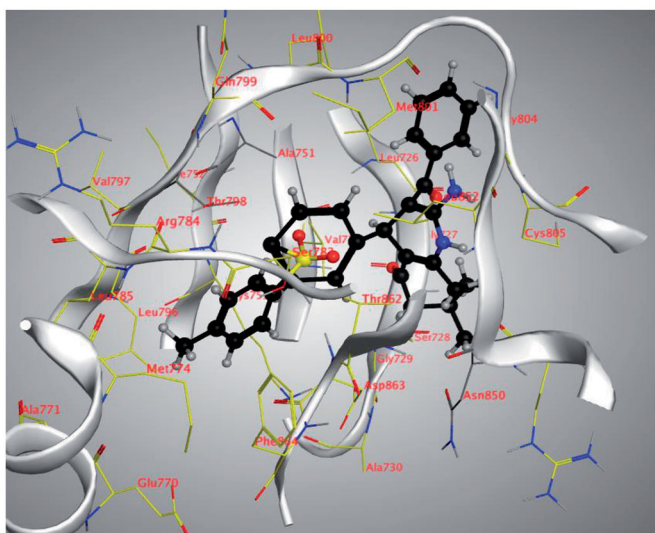
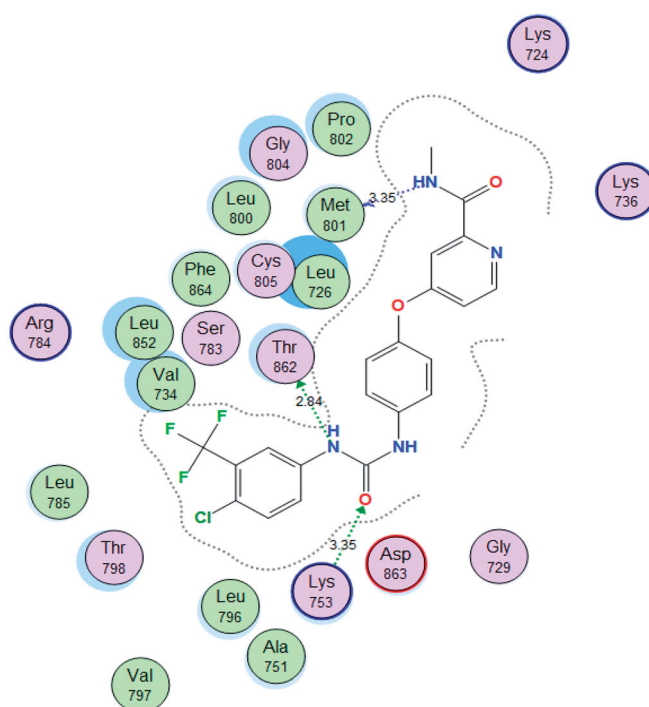
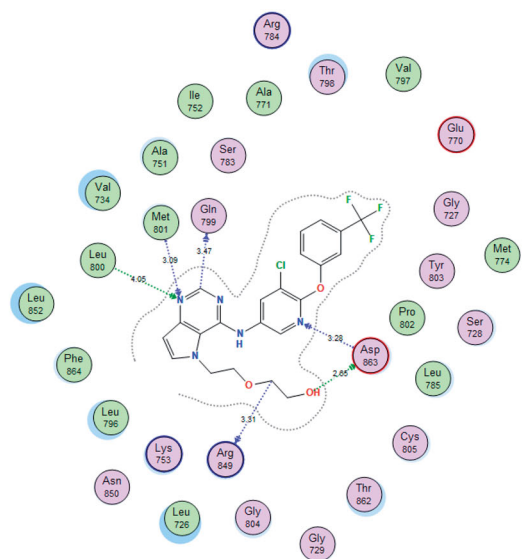
The molecular modelling studies were carried out using MOE (2019.0102) software. All minimisations were performed with MOE until an RMSD gradient of 0.1 kcal·mol<sup>-1</sup> Å<sup>-1</sup> with MMFF94x force field, and the partial charges were automatically calculated.

### 4.1. Human epidermal growth factor receptor 2 (HER2)

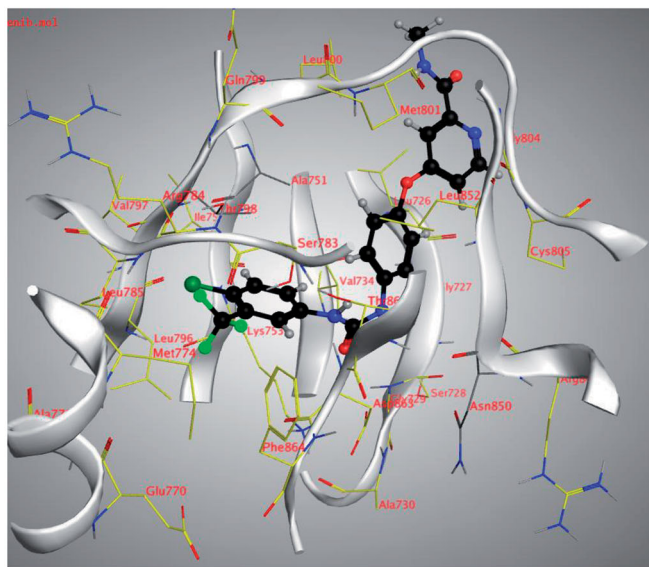
The X-ray crystallographic structure of human HER2 (HER2) co-crystallised with 2-{2-[4-({5-chloro-6-[3-(trifluoromethyl)phenoxy]pyridin-3-yl}amino)-5H-pyrrolo[3,2-d]pyrimidin-5-yl]ethoxy}ethanol

**Table 6.** Docking data of compound **4j** in the active site of HER2.

Compound	S (kcal/mol)	Amino acids	Interacting groups	Type of interaction	Length
<b>4j</b>	-17.3597	Gln799	CH (Pyrimidine)	Electrostatic	3.47
		Leu800	N (Pyrimidine)	H-bond acceptor	4.05
		Met801	N (Pyrimidine)	H-bond acceptor	3.09
		Arg849	CH <sub>2</sub>	Electrostatic	3.31.2021
		Asp863	OH	H-bond donor	2.65
<b>Sorafenib</b>	-15.4085	Asp863	N (Pyridine)	H-bond acceptor	3.28
		Lys753	O (C=O)	H-bond acceptor	3.35
		Met801	NH (Amide)	H-bond donor	3.25
		Thr862	NH (Urea)	H-bond donor	2.84

**Figure 9.** 2D and 3D diagram of compound **4j** interactions within HER2 binding site.

(03Q) (PDB ID: 3PP0) was downloaded from the protein data bank (<https://www.rcsb.org/structure/3PP0>). For each co-crystallised enzyme, water molecules and ligands that are not involved in the binding were removed. The protein was prepared for the docking study using *Protonate 3D* protocol in MOE with default options. The co-crystallised ligand (03Q) was used to define the binding site for docking. Triangle Matcher placement method and London dG scoring function were used for docking.

**Figure 10.** 2D and 3D diagram of compound Sorafenib interactions with HER2 binding site.

Through examination of the binding interactions of 03Q to the active site of the enzyme, it shows strong bond interactions with Gln799, Leu800, Met801, Arg849, and Asp863 (Figure 7).

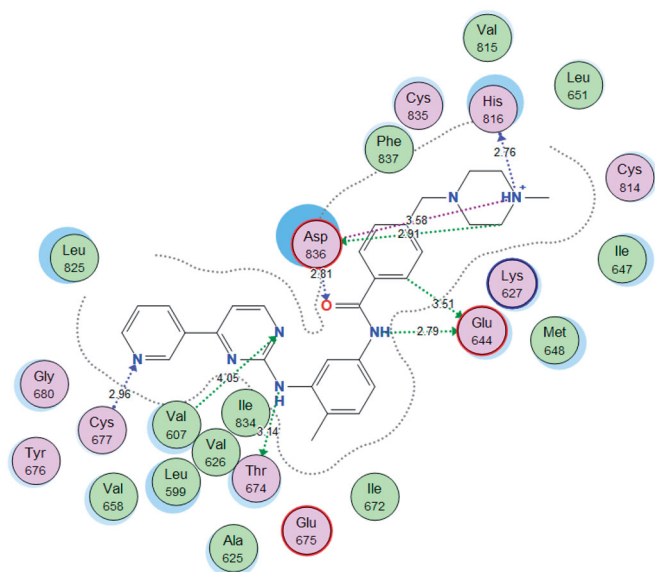


Figure 11. 2D interactions of imatinib within PDGFR- $\alpha$  active site.

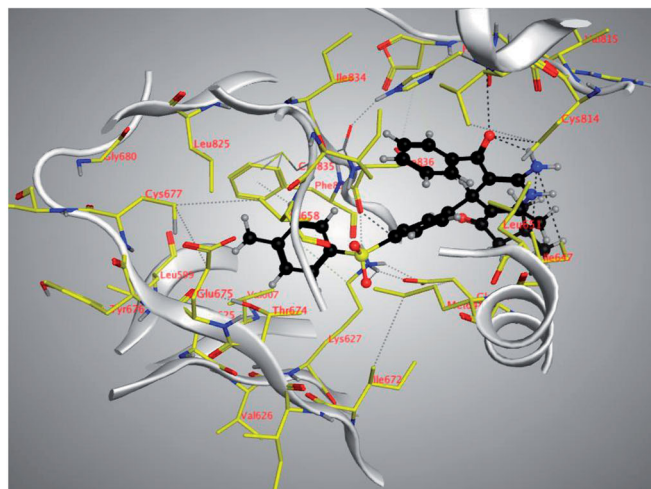
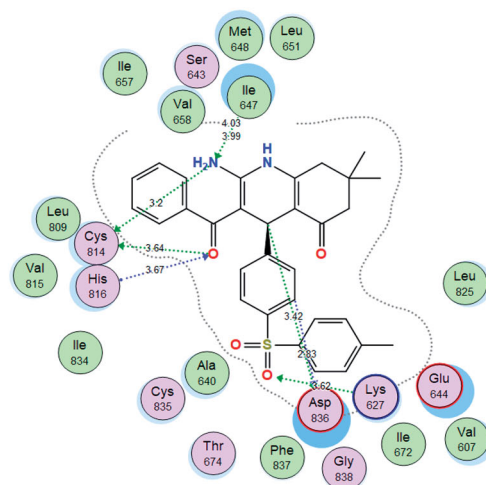


Figure 13. 2D and 3D diagram of compound 4j interactions within PDGFR- $\alpha$  binding site.

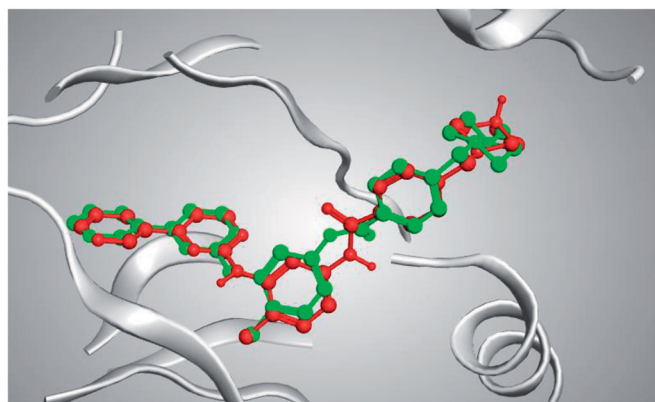


Figure 12. 3D representation of the superimposition of the co-crystallised (red) and the docking pose (green) of imatinib in the active site of PDGFR- $\alpha$ .

The docking setup was first validated by self-docking the co-crystallised ligand (30Q) in the vicinity of the enzyme's binding site. The docking score (*S*) was  $-17.1413$  kcal/mol, and the root means square deviation (RMSD) was  $0.14339$  Å (Figure 8).

The 4j compound showed high energy binding score ( $-17.3597$  kcal/mol.) similar to that of the co-crystallised ligand and higher than Sorafenib. Moreover, it showed good binding interactions with the amino acids in the active site of the receptor. The results are summarised in Table 6 and Figures 9 and 10.

Table 7. Docking results of compound 4j in the active site of PDGFR- $\alpha$ .

Compound	<i>S</i> (kcal/mol)	Amino acids	Interacting groups	Type of interaction	Length
4j	-13.2171	Lys627	O (S = O)	H-bond acceptor	3.62
		Ile647	NH <sub>2</sub>	H-bond acceptor	3.99
		Cys814	NH <sub>2</sub>	H-bond donor	3.20
		Cys814	O (C = O)	Electrostatic	3.64
		His816	O (C = O)	H-bond acceptor	3.67
		Asp836	CH (Phenyl)	Electrostatic	2.83
		Asp836	CH	Electrostatic	3.42
Sorafenib	-13.0476	Glu644	NH	H-bond donor	2.87
		Glu644	NH	H-bond donor	3.26
		Met648	NH	H-bond acceptor	4.05
		Cys677	O (C = O)	H-bond acceptor	3.00
		Cys814	Cl	Halogen bond	3.97
		Asp836	O (C = O)	H-bond acceptor	2.88

#### 4.2. Platelet-derived growth factor receptor $\alpha$ (PDGFR- $\alpha$ )

The X-ray crystallographic structure of human PDGFRA co-crystallised with Imatinib (PDB ID: 6JOL) was downloaded from the protein data bank (<https://www.rcsb.org/structure/6JOL>). For each co-crystallised enzyme, water molecules and ligands that are not involved in the binding were removed. The protein was prepared for the docking study using *Protonate 3D* protocol in MOE with default options. The co-crystallised ligand (imatinib) was used to define the binding site for docking. Triangle Matcher placement method and London dG scoring function were used for docking.

By examining the binding interactions of imatinib to the enzyme's active site, it shows strong bond interactions with Val607, Glu644, Thr674, Cys677, His816, and Asp836 (Figure 11).

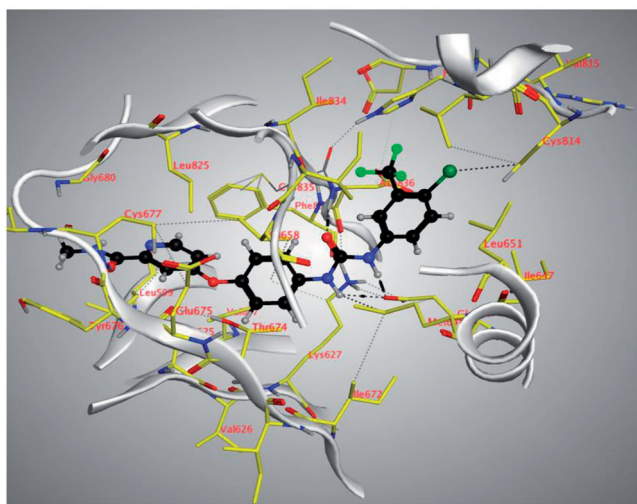
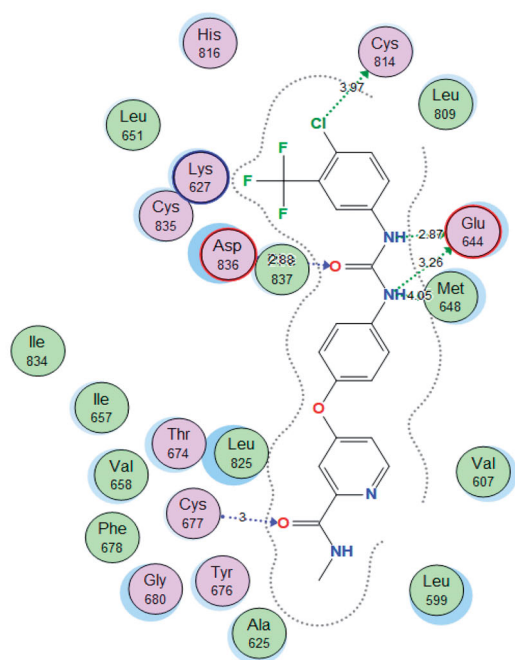


Figure 14. 2D and 3D diagram of Sorafenib interactions within PDGFR- $\alpha$  binding site.

The docking setup was first validated by self-docking the co-crystallised ligand (imatinib) in the vicinity of the enzyme's binding site. The docking score (S) was  $-18.0520$  kcal/mol, and RMSD was  $0.6983$  Å (Figure 12).

The **4j** compound showed a similar energy binding score to that of Sorafenib. It exhibited good binding interactions with the amino acid in PDGFR- $\alpha$  active site. The results are summarised in Table 7 and Figures 13 and 14.

## 5. Conclusion

A new class of 4,6,7,8-tetrahydroquinolin-5(1*H*)-one-based derivatives has been green synthesised as anti-breast cancer (MCF-7) agents of potential multi-targeting RTKs. The compounds **4a–i** were examined as cytotoxic agents against MCF-7 cancer cells using MTT assay utilising staurosporine as a standard drug. The compounds **4b**, **4e**, **4j**, and **4k** appeared as the most promising cytotoxic candidates. That revealing a more potent inhibiting effect than staurosporine, displaying  $IC_{50}$  values ranging from  $0.002$  to  $0.004$   $\mu$ M vs.  $IC_{50}$  value of

staurosporine,  $0.007$   $\mu$ M. The safety profile of the latter derivatives was evaluated against the normal WI38 cells. The compounds **4b** and **4j** appeared as the safest agents on the normal cells. Furthermore, the compound **4b**, **4j** were selected as representative examples to evaluate their suppression activity against EGFR, HER-2, PDGFR- $\alpha$ , and VEGFR-2 protein kinases. The compound **4j** investigated potent multi-targeting inhibitory activity in comparison with Sorafenib. In addition, the biological evidence revealed that the compound **4j** caused a marked apoptotic degree with a necrosis percentage 4.2%, leading to cell cycle disruption at G2/M phase in MCF-7 cancer cells. Accordingly, the new derivatives bearing 4,6,7,8-tetrahydroquinolin-5(1*H*)-one scaffold could be considered primary nuclei for further structural optimisation to get more potent, selective, and safer anticancer candidates. A molecular docking study was found in complete agreement with the obtained experimental results.

## Acknowledgements

The authors, therefore, gratefully acknowledge DSR technical and financial support. The authors would like to thank Dr. Mostafa. A. Hussein, at chemistry department, King Abdulaziz University, for his informative discussion, especially in the Docking studies.

## Disclosure statement

No potential conflict of interest was reported by the author(s).

## Funding

This work was supported by the Deanship of Scientific Research (DSR) at King Abdulaziz University, Jeddah, Saudi Arabia, under grant no. DF-838-130-1441.

## ORCID

Mohamed Mokhtar  <http://orcid.org/0000-0002-0594-7207>

Nesreen S. Ahmed  <http://orcid.org/0000-0001-9136-9986>

Dina Bakhotmah  <http://orcid.org/0000-0001-6651-7932>

## References

- Torre LA, Islami F, Siegel RL, et al. Global cancer in women: burden and trend, *Cancer Epidemiol. Biomark Prev* 2017;26: 444–57.
- Siegel RL, Miller KD, Jemal A. Cancer statistics, 2018. *Cancer J Clin* 2018;68:7–30.
- Shyamsivappan S, Vivek R, Saravanan A, et al. A novel 8-nitro quinoline-thiosemicarbazone analogues induces G1/S & G2/M phase cell cycle arrest and apoptosis through ROS mediated mitochondrial pathway. *Bioorg Chem* 2020;97: 103709.
- Yang K, Yang JQ, Luo SH, et al. Synthesis of N-2(5H)-furanonyl sulfonyl hydrazone derivatives and their biological evaluation in vitro and in vivo activity against MCF-7 breast cancer cells. *Bioorg Chem* 2021; 107:104518.
- Verma SK, Ratre P, Jain AK, et al. De novo designing, assessment of target affinity and binding interactions against aromatase: discovery of novel leads as anti-breast cancer agents. *Struct Chem* 2021;32:847–58.
- Robinson DR, Wu YM, Lin SF. The protein tyrosine kinase family of the human genome. *Oncogene* 2000;19:5548–57.

7. Myers SH, Brunton VG, Unciti-Broceta A. AXL inhibitors in cancer: a medicinal chemistry perspective. *J Med Chem* 2016;59:3593–608.
8. Ségaliny AI, Tellez-Gabriel M, Heymann MF, Heymann D. Receptor tyrosine kinases: characterisation, mechanism of action and therapeutic interests for bone cancers. *J Bone Oncol* 2015;4:1–12.
9. Sarukhanyan E, Shityakov S, Dandekar T. Rational drug design of Axl tyrosine kinase type I inhibitors as promising candidates against cancer. *Front Chem* 2020;7:920.
10. Guo T, Ma S. Recent advances in the discovery of multitargeted tyrosine kinase inhibitors as anticancer agents. *ChemMedChem* 2021;16:600–20.
11. Roskoski R. Jr. Properties of FDA-approved small molecule protein kinase inhibitors: a 2020 update. *Pharmacol Res* 2020;152:104609.
12. Broekman F, Giovannetti E, Peters GJ. Tyrosine kinase inhibitors: multi-targeted or single-targeted? *World J Clin Oncol* 2011;2:80–93.
13. Raghavendra NM, Pingili D, Kadasi S, et al. Dual or multi-targeting inhibitors: the next generation anticancer agents. *Eur J Med Chem* 2018;143:1277–300.
14. Govindachari TR, Viswanathan N. The stem bark of *Mappia foetida*, a tree native to India, has proved to be another source significant for the isolation of camptothecin. *Phytochemistry* 1972;11:3529–31.
15. Martorana A, Monica GL, Lauria A. Quinoline-based molecules targeting c-met, EGF, and VEGF receptors and the proteins involved in related carcinogenic pathways. *Molecules* 2020;25:4279.
16. Marella A, Tanwar OP, Saha R, et al. Quinoline: a versatile heterocyclic. *Saudi Pharm J* 2013;21:1–12.
17. Afzal O, Kumar S, Haider MR, et al. A review on anticancer potential of bioactive heterocycle quinoline. *Eur J Med Chem* 2015;97:871–910.
18. Musiol R. An overview of quinoline as a privileged scaffold in cancer drug discovery. *Expert Opin Drug Discov* 2017;12:583–97.
19. Cortes JE, Gambacorti-Passerini C, Deininger MW, et al. Bosutinib versus imatinib for newly diagnosed chronic myeloid leukemia: results from the randomized BFORE trial. *J Clin Oncol* 2018;36:231–7.
20. Zschäbitz S, Grüllich C. Lenvatinib: a tyrosine kinase inhibitor of VEGFR 1-3, FGFR 1-4, PDGFR $\alpha$ , KIT and RET. *Recent Result Cancer Res* 2018;211:187–98.
21. Markowitz JN, Fanher KM. Cabozantinib: a multitargeted oral tyrosine kinase inhibitor. *Pharmacotherapy* 2018;38:357–69.
22. Deeks ED. Neratinib: first global approval. *Drugs* 2017;77:1695–704.
23. Alafeefy AM. Design, synthesis, and antitumor screening of certain novel tetrahydroquinoline sulfonamides. *J Enzyme Inhib Med Chem* 2015;30:189–94.
24. Pacchiano F, Carta F, McDonald PC, et al. Ureido-substituted benzenesulfonamides potentially inhibit carbonic anhydrase IX and show antimetastatic activity in a model of breast cancer metastasis. *J Med Chem* 2011;54:1896–902.
25. Takacova M, Holotnakova T, Barathova M, et al. Src induces expression of carbonic anhydrase IX *via* hypoxia-inducible factor 1. *Oncol Rep* 2010;23:869–74.
26. Maresca A, Temperini C, Vu H, et al. Non-zinc mediated inhibition of carbonic anhydrases: coumarins are a new class of suicide inhibitors. *J Am Chem Soc* 2009;131:3057–62.
27. Maresca A, Temperini C, Pochet L, et al. Deciphering the mechanism of carbonic anhydrase inhibition with coumarins and thiocoumarins. *J Med Chem* 2010;53:335–44.
28. Hou Y, Shang C, Wang H, Yun J. Isatin-azole hybrids and their anticancer activities. *Arch Pharm (Weinheim)* 2020;353:e1900272.
29. Ding Z, Zhou M, Zeng C. Recent advances in isatin hybrids as potential anticancer agents. *Arch Pharm (Weinheim)* 2020;353:e1900367.
30. Fortin S, Bérubé G. Advances in the development of hybrid anticancer drugs. *Expert Opin Drug Discov* 2013;8:1029–47.
31. Mokhtar M, Saleh TS, Ahmed NS, Al-Bogami AS. A green mechanochemical one-pot three-component domino reaction synthesis of polysubstituted azoloazines containing benzofuran moiety: cytotoxic activity against HePG2 cell lines. *Polycyclic Aromatic Compounds* 2020;40:594–608.
32. Mokhtar M, Alhashedi BFA, Kashmery HA, et al. Highly efficient nanosized mesoporous cumgal ternary oxide catalyst for nitro-alcohol synthesis: ultrasound-assisted sustainable green perspective for the Henry reaction. *ACS Omega* 2020;5:6532–44.
33. Althabaiti NS, Al-Nwaiser FM, Saleh TS, Mokhtar M. Ultrasonic-assisted Michael addition of arylhalide to activated olefins utilizing nanosized CoMgAl-layered double hydroxide catalysts. *Catalysts* 2020;10:220.
34. Al-Bogami AS, Saleh TS, Moussa TAA. Green synthesis, antimicrobial activity and cytotoxicity of novel fused pyrimidine derivatives possessing a trifluoromethyl moiety. *ChemistrySelect* 2018;3:8306–11.
35. Alghamdi KS, Ahmed NSI, Bakhotmah D, Mokhtar M. Chitosan decorated copper nanoparticles as efficient catalyst for synthesis of novel quinoline derivatives. *J Nanosci Nanotechnol* 2020;20:890–9.
36. Ulman A, Urankar E. A novel synthesis of 4-[alkyl(aryl)sulfonyl]benzaldehydes: alkyl(aryl)sulfinate anion as a nucleophile in aromatic substitutions. *J Organ Chem* 1989;54:4691–2.
37. Yuan YQ, Guo SR. A mild and efficient synthesis of aryl sulfones from aryl chlorides and sulfinic acid salts using microwave heating. *Synlett* 2011;2011:2750–6.
38. Hosamani KM, Reddy DS, Devarajegowda HC. Microwave-assisted synthesis of new fluorinated coumarin-pyrimidine hybrids as potent anticancer agents, their DNA cleavage and X-ray crystal studies. *RSC Adv* 2015;5:11261–71.
39. Amin KM, Syam YM, Anwar MM, et al. Synthesis and molecular docking study of new benzofuran and furo[3,2-g]chromone-based cytotoxic agents against breast cancer and p38 $\alpha$  MAP kinase inhibitors. *Bioorg Chem* 2018;76:487–500.
40. Abbas HS, Abd El-Karim SS. Design, synthesis and anticervical cancer activity of new benzofuran-pyrazol-hydrazono-thiazolidin-4-one hybrids as potential EGFR inhibitors and apoptosis inducing agents. *Bioorg Chem* 2019;89:103035.
41. Panda SS, Liaqat S, Girgis AS, Samir A, et al. Novel antibacterial active quinolone-fluoroquinolone conjugates and 2D-QSAR studies. *Bioorg Med Chem Lett* 2015;25:3816–21.
42. Nossier ES, Abd El-Karim SS, Khalifa NM, et al. Kinase inhibitory activities and molecular docking of a novel series of anticancer pyrazole derivatives. *Molecules* 2018;23:3074.
43. Puratchikody A, Sriram D, Umamaheswari A, Irfan N. 3-D structural interactions and quantitative structural toxicity studies of tyrosine derivatives intended for safe potent inflammation treatment. *Chem Cent J* 2016;10:24.

44. Mason TJ, Tiehm A, *Advances in sonochemistry, volume 6: ultrasound in environmental protection*. Amsterdam, Netherlands: Elsevier Science; 2001:145.
45. Shah YT, Pandit AB, Moholkar VS. *Cavitation reaction engineering*. New York (NY): Plenum Publishers; 1999.
46. Mosmann T. Rapid colorimetric assay for cellular growth and survival: application to proliferation and cytotoxicity assays. *J Immunol Methods* 1983;65:55–63.
47. Vistica DT, Skehan P, Scudiero D, et al. Tetrazolium-based assays for cellular viability: a critical examination of selected parameters affecting formazan production. *Cancer Res* 1991;51:2515–20.
48. Edmondson JM, Armstrong LS, Martinez AO. A rapid and simple MTT-based spectrophotometric assay for determining drug sensitivity in monolayer cultures. *J Tissue Cult Meth* 1988;11:15–7.
49. Anwar MM, Abd El-Karim SS, Mahmoud AH, et al. A comparative study of the anticancer activity and PARP-1 inhibiting effect of benzofuran–pyrazole scaffold and its nano-sized particles in human breast cancer cells. *Molecules* 2019;24:2413.
50. Liu F, Liu D, Yang Y, Zhao S. Effect of autophagy inhibition on chemotherapy-induced apoptosis in A549 lung cancer cells. *Oncol Lett* 2013;5:1261–5.
51. MacLachlan TK, Sang N, Giordano A. Cyclins, cyclin-dependent kinases and cdk inhibitors: implications in cell cycle control and cancer. *Crit Rev Eukaryot Gene Expr* 1995;5: 127–56.